

Multifractal Methods for Asset Pricing

Daniel Leibovici

June 26, 2018



Finance Major

Master Thesis

Supervisor: Professor Nicolas Vieille

Contents

1	Acknowledgements	3
2	Introduction	4
3	The use of Multifractals in Finance	5
3.1	The limits of classic financial models	5
3.2	Fractal Finance	5
3.3	Properties of the multifractals	8
4	Mathematical foundations	10
4.1	Fractal sets and Hausdorff dimension	10
4.2	Multifractal Measures	14
4.3	The Multifractal formalism	15
4.4	Multifractal processes	17
5	Multifractal Models	18
5.1	The Markov-Switching Multifractal in Discrete Time (MSM)	18
5.2	The Multifractal Model of Asset Returns (MMAR)	20
5.3	Continuous-Time MSM	26
6	Practical applications	31
6.1	Calibrating the Markov-Switching Multifractal in Discrete Time	31
6.2	Calibrating the Continuous Time MSM	35
7	Conclusion	38
8	Appendix	40
8.1	Appendix 1: The Hausdorff dimension of the Cantor Set	40
8.2	Appendix 2: Moment-scaling property of the log-price process for the MMAR and the MSM in Continuous time	40

1 Acknowledgements

I would like to express my gratitude to Professor Nicolas Vieille, my thesis supervisor, for his guidance, availability and useful critiques for this master thesis.

I would also like to extend my thanks to the staff of the HEC Library for their precious help in the research of publications and data to help build this master thesis.

I wish to thank the academic team from the Finance Major who helped me understand the financial concepts which this article deals with, as well as my friends from the Major and the MIF for their support.

Finally, I wish to thank my parents for their unfailing support and their efforts that allow me to pursue my dreams in life.

Abstract

As the repetition of extreme financial events such as the 2008 global financial crisis has pointed out, the study of the volatility of asset prices is a key topic in finance. Classic models such as Black-Scholes have often occulted the question, sometimes assuming volatility to remain constant, and treat extreme phenomena as outliers. However methods revolving around Fractal geometry, which were developed by Benoît Mandelbrot, allow to take into account these events. These foundations allowed to develop models that harvest the scaling properties of fractal geometry to analyze financial series. This thesis presents Multifractal models, which allow a multiplicity of scaling behaviors and help reproduce empirical features of the volatility such as clustering and long-memory. Using different methods, one can calibrate this models to study real data, such as foreign exchange rates.

2 Introduction

As extreme and frequent market behaviors have shown it, classic financial models based on the log-normal distribution and the independence of the returns do not seem to be verified empirically. The *fat tails* observed in the actual distribution of the log-returns are not well explained by some of the most widely used models such as Black-Scholes. Moreover volatility, one of the biggest topics in finance nowadays, appears to show properties of persistence in time: periods of high and low volatility tend to last and to alternate.

Nevertheless, mathematicians such as Benoît Mandelbrot looked for patterns in order to try to find some order in this apparent chaos. Fractal geometry, a field of mathematics concerned with the study of very irregular curves, seemed to be very promising in this endeavor. Mandelbrot's work, combined with the development of computational capacities in the 1960s and 1970s, allowed to analyze very large sets of data and to highlight some of these patterns. Fractal analysis emphasized the scaling properties of the moments of the log-returns, and help better understand the thematics of clustering in volatility. These studies not only allowed the field of Fractal Geometry to develop, but are also the cement of many financial models later proposed by other mathematicians and economists, such as Calvet and Fisher's Markov Switching Multifractal model.

In the first part of this paper, we will discuss how Fractal Finance allows to model phenomena observed empirically, but that classic models fail to explain. In particular, we will explain why *Multifractal* models and their properties are useful in the analysis of financial series.

Afterwards in the second part, we will delve into the definition of fractals from a mathematical point of view. We will also the Hausdorff dimension, a fundamental object in fractal analysis. Eventually, we will focus on the definition of multifractal processes and their properties.

We will then describe three multifractal models: the Markov-Switching Multifractal models in discrete and continuous time (MSM), and the Multifractal Models of Asset Returns (MMAR). We will define these models from a mathematical point of view and analyze their properties thanks to numerical simulations.

Finally, we will use the MSM models on real data (foreign exchange rates) and explain how to calibrate these models, either by maximizing a log-likelihood function (discrete time model) or by using the mathematical properties of the multifractal processes in the form of the multifractal spectrum (continuous time model).

3 The use of Multifractals in Finance

3.1 The limits of classic financial models

Major financial events, such as the *Black Monday* crash of 1987, the *Tech bubble burst* of 2000 or the *bear market* between 2007 and 2009 in the United States, during which the Dow Jones lost more than 20% of its value, occur at too high a frequency for them to be explained by classic financial models.

This problem is better known as the problem of fat tails. Classic financial models are based on the assumptions that the returns follow a log-normal distribution. They are inspired by the work of the French mathematician Louis Bachelier at the beginning of the XX^{th} century, which introduced the use of the Brownian motion in finance. However, the assumed distributions don't seem to capture the reality, particularly because extreme events occur too often. Thus, the tails of the observed distribution are much thicker than they are expected to be following this theory.

A way practitioners used to deal with this discrepancy between theory and practice was simply to ignore these extreme behaviors and treat them as outliers. However, these extreme price swings are frequent enough to be considered as the norm, and not as aberrations that can be overlooked. Bubbles, crashes and reversals are characteristic of markets.

Another assumption that is often made is the independence of the return process. However we often observe that periods of high volatility tend to persist: days of large price movements are often followed by other large price movements, whether they are crashes or reversals. Similarly, periods of calm tend to last for long extents of time (which is why the log-normal distribution of returns is appealing, and some models like Black-Scholes even consider the volatility to be constant). We say that volatility clusters, and this empirical observation strongly contradicts the independence of the return process.

3.2 Fractal Finance

It became clear that the Brownian model had too many flaws to accurately describe the financial series. Despite giving a good representation of the distribution of the returns 95% of the time, some price variations are too chaotic and repeat themselves too often to believe in a Gaussian distribution of log-returns

Should analysts and economists just settle for this partial version of the truth, or just consider that the financial markets are too chaotic to be described by mathematical models ?

It may still be possible to find some order in the roughness of the financial series. For mathematicians such as Benoît Mandelbrot, the father of fractal geometry, it was natural to try to apply the techniques of fractal analysis to financial series. These methods consist in the study of the repetition of patterns that display similarities at different scales. One of the most famous fractal objects is the snowflake, which has a shape pattern that reproduces itself as we "zoom" in any part of it. It is mathematically represented that the Von Koch curve, that we will describe again later, see Figure 4. We call such an object self-similar, because it is entirely made of identical but rescaled reproductions of itself : the snowflake shape keeps repeating itself as we zoom in any area of the snowflake. Since fractals are useful in describing very chaotic curves such as mountain lines or coastlines, one could indeed use this mathematical object to have a better understanding of financial series. Since, unlike for the snowflake, the coordinate axis matter for the financial series (indeed, we represent prices in function of the time and we couldn't mix these different units), we do not talk about self similarity when analyzing financial series but about self affinity: the transformations that allow to observe the repetition of patterns at different scales include affine transformations but exclude rotations.

A first approach to try to replicate the graph of financial series is to divide our global time interval into equal subintervals, and represent trends over these intervals. We call these trends generators. As a second step, we subdivide again the subintervals into smaller intervals, and repeat the pattern of our generator at this new scale. We can repeat this process several times by interpolating a new curve shaped like the generator between the points we already had from the previous steps, and obtain a curve that looks like the graph of the evolution of a stock price. By applying this method, we are creating a *unifractal* process: at each step the curve is lengthened by the same ratio, since we interpolate the same compressed generator between the points that are already built. See Figure 1 for more details.

1 THREE-PIECE FRACTAL GENERATOR (*top*) can be interpolated repeatedly into each piece of subsequent charts (*bottom three diagrams*). The pattern that emerges increasingly resembles market price oscillations. (The interpolated generator is inverted for each descending piece.)

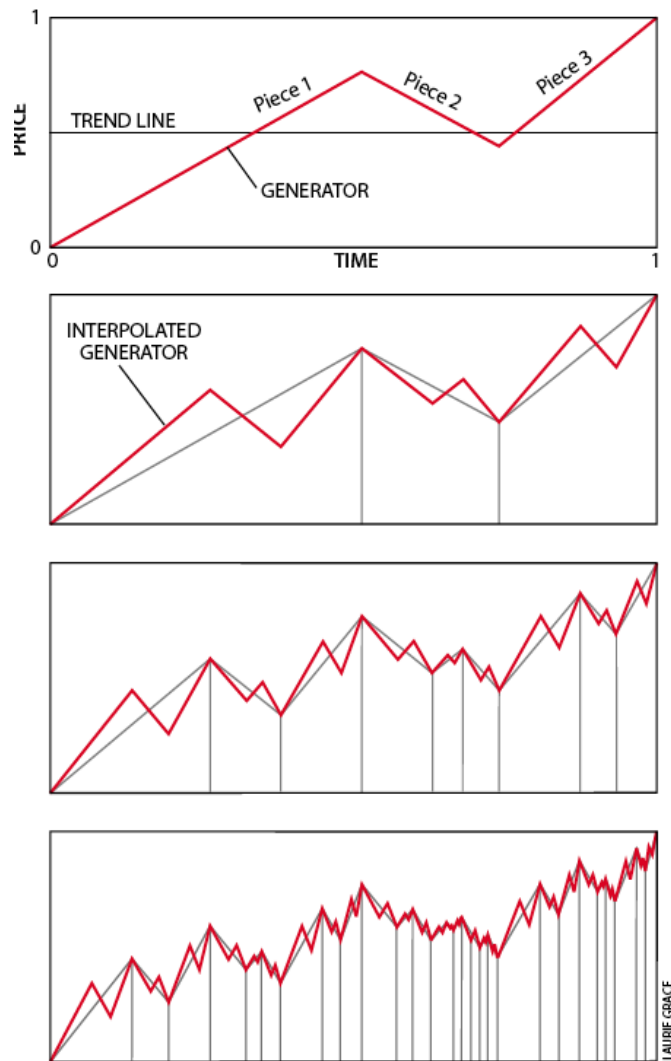
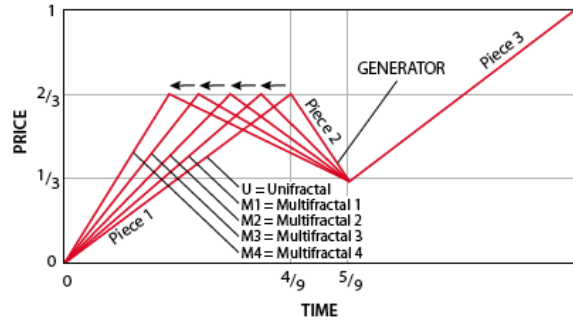
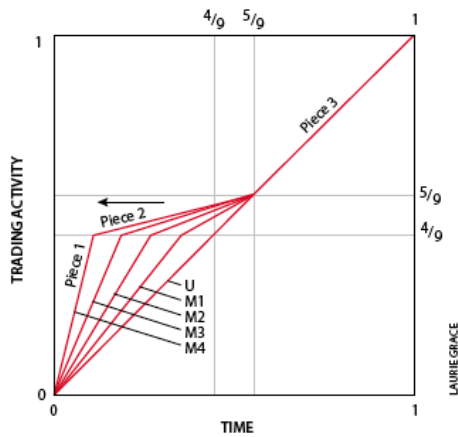


Figure 1

2 MOVING A PIECE of the fractal generator to the left ...



3 ... causes the same amount of market activity in a shorter time interval for the first piece of the generator and the same amount in a longer interval for the second piece ...



4 ... Movement of the generator to the left causes market activity to become increasingly volatile.

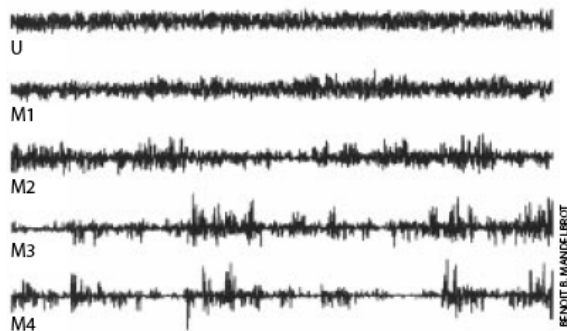


Figure 2

This unifractal representation implies that the trading activity takes place at the same *pace* during any time interval: there are no slow downs or acceleration. By randomly stretching or compressing a piece of the generator at each step, we can add a new layer of complexity to our model. This modification is equivalent to randomly stretching or compressing the horizontal time axis, and is a very important feature in finance, as it is done one Figure 2. Indeed, accelerations and slow-downs of the trading activity are very common, during a crash or during a very calm period for instance. On a daily basis, the activity is also much more intense during the opening and the closing of the market than in the middle of the day. By integrating into our model a certain number of modes in which this piece of the generator line can be rescaled (it could also be rescaled in a countable or a continuum number of ways, as we will see later), we transformed our unifractal model in a *multifractal* model.

As we have just discussed, the use of fractals to describe financial series and try to replicate them is quite intuitive when we look at the graphs, by considering the same kind of shapes are repeated at different scales, with possibly different ratios of compression or dilatation that are representative of the acceleration or slow-down of the activity. Nevertheless, in this we will adopt a different perspective on the use of this fractal analysis. Instead of focusing directly on the graph, we will focus on the variations of the process (whether it is the returns, or the log-price). More precisely, we will examine the intensity of these variations on short periods of time, and the frequency at which a certain intensity repeats itself. These views are in fact very closely related, since looking for a very intense variation of the process is equivalent to searching for intervals of time in which a piece of the generator line was very compressed, thus corresponding to a period of high trading activity.

Our goal will thus be to model the variations of volatility in time, thanks to processes called *multifractal processes*, that allow to represent these time accelerations and slow-downs. These time-deformations are related to variations in trading activity, which in turn can be explained economically by a superposition of cycles with different time-length, as we will detail later. Accelerations and slow-down of the activity are the essence of the variation in volatility, and analyzing how these deformations are organized will allow us to understand how volatility clusters.

3.3 Properties of the multifractals

The use of multifractal models to analyze financial series has the benefit of displaying some important properties that the standard Black-Scholes model has overlooked, and that nevertheless have deep economic interpretations. The motivation to look beyond this standard model came from its inability to predict some extreme variations in prices, that it judged to be much rarer than they actually are. Moreover, this model assumed independence in the price changes between different time periods, which is observably untrue: large price changes tend to be followed by other large price changes, and this is also the case for small price changes.

We say that volatility tends to cluster: periods with high volatility alternate with periods of low volatility, and the magnitude of the price changes tends to persist during those periods. This phenomenon is widely observed in the financial markets. Indeed, periods of crashes during which the value of a stock can drop dramatically several days consecutively before intensely rebounding during a correction often alternate with longer periods of calm, with a very low volatility. An economic interpretation behind these observations is that the market is subject to stacked economic cycles, that have different periods of time and different characteristics. As we will see later when discussing the Markov-Switching Multifractal models, at a given time these different cycles could be in the middle of a tumultuous state of high volatility, or a rather calm state of low volatility. The volatility of the market at a given time is obtained by aggregating the volatilities implied by these different cycles. Thus if the majority of the cycles with a long period are in a state of low volatility, then overall the magnitude of the price changes in the market should be low, even if spikes can be intermittently provoked by very short cycles (such as the default of a given company that won't have a lasting impact on the market). Inversely, if the majority of the long period cycles are in a state of high volatility, such as during an important financial crisis, then the market will remain very volatile for an extended period of time.

Such a model can thus explain the fat tails encountered in practice in the financial markets, since it allows for periods of high volatility to last more, and to come back periodically.

Note that in this paper, we will focus on the study of exchange rate between strong currencies. Thus, the direction of the variation of the spot exchange rate doesn't really matter : we don't expect it to decrease more dramatically than it would increase, as we do for stocks, because a

negative shock could be happening on either one of the currencies. Thus we don't expect the returns to be skewed in any direction.

Thus it is important to have a model that displays this volatility clustering property, and we will commit to show that the models described in this paper indeed display this property. From this volatility clustering results a second fundamental property of financial series that was overlooked by the traditional models : the property of *long memory*. As we have stated before, the independence of the returns at different moments in time, as implied by the Black-Scholes model, is very unrealistic. Indeed, as volatility tends to cluster, the squared returns are noticeably correlated over short periods of time. More, we can show that the autocorrelation between the squared log-returns, i.e. the correlation between the squared log-returns separated by a certain lag, diminishes hyperbolically with the lag, that is as a power of the inverse of the lag. This decay is said to be slow, when compared to an exponential decay. Mathematically, these decays are defined by :

hyperbolic decay : there exists $a > 0$ such that $autocorrelation = lag^{-a}$

exponential decay : there exists $0 < a < 1$ such that $autocorrelation = a^{lag}$

Thus we expect the autocorrelation levels to be significant also for long lags. We will show that this property holds for the multifractal models we will study.

4 Mathematical foundations

4.1 Fractal sets and Hausdorff dimension

In his research, Mandelbrot developed methods in order to study sets with very irregular shapes. These sets include galaxies, snowflakes or coastlines. They display very bizarre characteristics such as coastlines with infinite length, or snowflakes with infinite surface area. Moreover, characteristics of the set at a certain level of magnification are preserved at different levels of magnification apart from a scale factor. We refer to these sets as self-similar.

These examples may seem hard to visualize without a precise mathematical definition. We will study two examples that will help us get a grasp of the underlying concept of fractals, and introduce the Hausdorff dimension.

4.1.1 Examples of Fractal Sets

We will first introduce the middle Cantor set. It is obtained by performing sequentially the same transformations at different scales on a sequence of sets, initially starting with the unit segment. Let E_0 be the unit segment. E_1 is obtained from E_0 by removing its middle third. Thus, E_1 is composed of two segments : $[0, \frac{1}{3}]$ and $[\frac{2}{3}, 1]$. Afterwards, E_2 is obtained from E_1 by performing the same transformation on the two segments composing it: their middle thirds are removed. Thus, the segment $[\frac{1}{9}, \frac{2}{9}]$ is removed from the segment $[0, \frac{1}{3}]$, and the segment $[\frac{7}{9}, \frac{8}{9}]$ is removed from the segment $[\frac{2}{3}, 1]$. For any integer $k \geq 2$, E_k is obtained by performing the same procedure on E_{k-1} . As k tends to infinity, E_k converges towards the middle third Cantor set F . This set seems to be hard to represent at a first glance. As at each construction step, the middle thirds of the previous segments were removed, we are not left with much when k tends to infinity. However, this set is far from being empty: we can see, quite straightforwardly, that points such as 0 and 1 belong to F . In fact, F is composed of an infinite, and even uncountable number of disjoint points.

We can show that the Lebesgue measure of the middle Cantor Set is zero. Indeed, at every step, the Lebesgue measure of E_k is $(\frac{2}{3})^k$: the length of E_0 is 1, the length of E_1 is $\frac{2}{3}$, and for every $k \geq 2$, E_k is obtained from E_{k-1} by removing the middle third of all the segments in E_{k-1} , thus E_k 's Lebesgue measure is two thirds of E_{k-1} 's.

Proving that F is uncountable is a very classic problem, which implies noticing that F is a mapping of the numbers in $[0,1]$ that only have 0s and 2s in their triadic expansions. By using Cantor's diagonal argument, this set can be shown to be uncountable, and so is F .

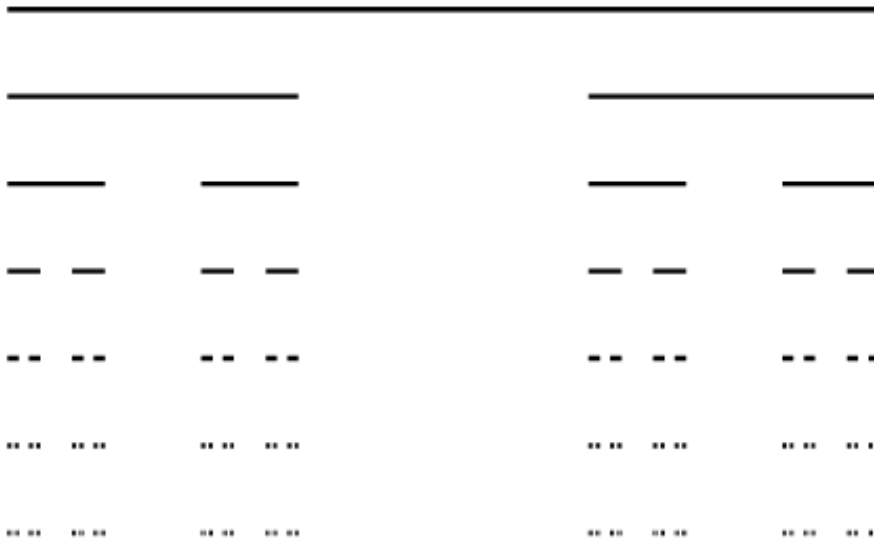


Figure 3: Construction of the middle Cantor set.

In this second example we will introduce the von Koch curve, which is the limit of a sequence of curves, obtained by performing the same transformations at different scales, at each step. We

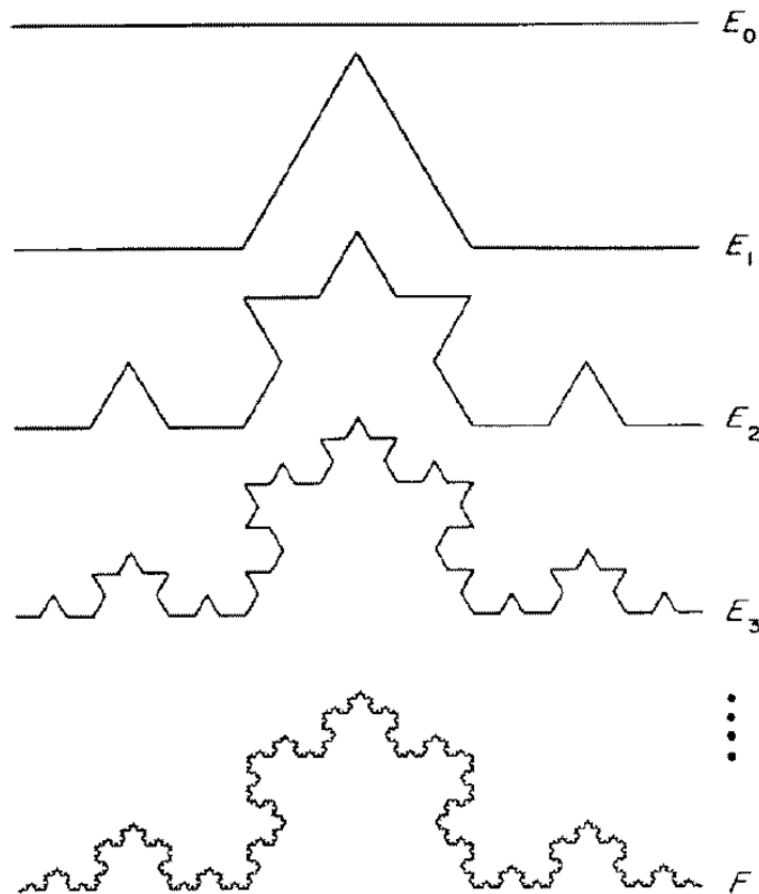


Figure 4: Construction of the von Koch curves, that converge towards a snowflake-shaped curve.

start from the segment E_0 , of unit length. We obtain E_1 by removing the middle third of E_0 and replacing it with the two other sides of an equilateral triangle built on the basis of this removed segment. Thus, E_1 is a curve composed of four segments: the first and third third of E_0 , and the two segments that replaced the second third of E_0 . For any integer $k \geq 2$, E_k is obtained by performing the same procedure on E_{k-1} : we replace each of the middle thirds of the 4^{k-1} segments of E_{k-1} by the two sides of the equilateral triangle built on the basis of the removed segment, and pointing towards the exterior of the built curve. As k tends to infinity, E_k converges towards the von Koch curve. Although we started with the unit segment, the von Koch curve obtained by taking the limit of the E_k actually has infinite length. Indeed, one can easily see that the length of E_k is $(\frac{4}{3})^k$: the length of E_0 is 1, the length of E_1 is $\frac{4}{3}$ (it is composed of two segments of length $\frac{1}{3}$ that have been left unchanged, and two segments also of length $\frac{1}{3}$ that replaced the middle third). By recursion, one can show that at every step, every segment is replaced by 4 segments with a total length of $\frac{4}{3}$ the length of the initial segment.

These examples are sets that are referred to as *Fractals*. They are objects that are too irregular to fit into classical geometric settings. They display properties of self-similarity that apply at different scales. In the examples that we have seen so far, these properties are geometrical, but they can also be statistical such as in financial series as we will see later on.

But how could we describe these very irregular objects, such as a coastline with infinite length, or a snowflake with infinite area? They are so irregular that they seem to spill out of their *natural* dimension: the von Koch curve, which is the limit of curves with more and more irregular straight lines, is far more complex than a 1-dimensional segment, and has infinite length as we have seen before. The middle Cantor set is also far more complex than a finite set of points, with dimension zero, since it is an infinite and uncountable set of points. Moreover, even though these two sets

are very irregular, they also are built in a very orderly way sequentially, and display self similar properties. Could we find an appropriate metric to better describe them ?

As hinted in the previous paragraph, the solution lies in the dimensionality of these objects. We will introduce the concept of Hausdorff dimension, that can be considered as an extension of the dimensions we usually consider. Hausdorff dimensions allow us to describe objects too irregular *to be contained* in what seems to be their *natural* dimension. For instance, the von Koch curve, with its infinite length, will have a Hausdorff dimension larger than one, actually comprised between one and two. Unlike countable sets of points that have a dimension zero, the middle Cantor set will have a Hausdorff dimension comprised between zero and one.

As a rule of thumb, one can calculate the Hausdorff for simple enough sets by doing the following: if the set is built recursively by the creation, at each step, of m copies of itself scaled by a factor r , then the Hausdorff dimension of the set is equal to $-\frac{\log m}{\log r}$. Thus, since at each step of the construction of the middle Cantor set, two copies of E_k scaled with a factor $1/3$ are created, the middle Cantor set has Hausdorff dimension $\frac{\log 2}{\log 3} \approx 0.63$. For the von Koch curve, at each step four copies are created scaled with a factor $1/3$, so the Hausdorff dimension of the von Koch curve is $\frac{\log 4}{\log 3} \approx 1.26$.

The two following parts give a more rigorous definition of the Hausdorff dimension, and show how to calculate it in the case of the middle Cantor set.

4.1.2 The Hausdorff measure

If U is a non-empty n -dimensional set of \mathbb{R}^n , the diameter of U is defined as $|U| = \sup_{(x,y) \in U^2} \{|x - y|\}$. If $\delta > 0$ and $\{U_i\}$ is a finite or countable collection of sets of diameter smaller than δ that cover U , i.e $U \subseteq \bigcup_{i=1}^{\infty} U_i$, we say that $\{U_i\}$ is a δ -cover of U .

Let F be a subset of \mathbb{R}^n and $s \in \mathbb{R}^{+*}$. We define

$$H_\delta^s(F) \equiv \inf \left\{ \sum_{i=1}^{\infty} |U_i|^s : \{U_i\} \text{ is a } \delta\text{-cover of } F \right\}$$

As δ decreases, the set of δ -covers of F also becomes reduced, so the infimum H_δ^s grows. We define the s -dimensional Hausdorff measure of F as follows :

$$H^s(F) = \lim_{\delta \rightarrow 0} H_\delta^s(F)$$

The limit exists for every subset F of \mathbb{R}^n , though it can be $+\infty$. H^s can be shown to be a measure. To within a constant multiple, it can be shown to be equal to the Lebesgue measure.

4.1.3 The Hausdorff dimension

Consider a F of \mathbb{R}^n , $\delta < 1$, and $s > 0$. For $t > s$, and any δ -cover U_i of F ,

$$\sum_{i=1}^{\infty} |U_i|^t < \delta^{t-s} \sum_{i=1}^{\infty} |U_i|^s$$

By taking the infima over all the δ -covers of F , we have $H_\delta^t(F) \leq \delta^{t-s} H_\delta^s(F)$. If we let δ tend to 0, we see that if $H^s(F) < \infty$, then $H^t(F) = 0$ for $t > s$. Thus, there is a critical value of s for which $H^s(F)$ jumps from ∞ to 0. This value is called the *Hausdorff dimension* of the set F .

$$\dim_H(F) = \inf \{s : H^s(F) = 0\} = \sup \{s : H^s(F) = \infty\}$$

$$\text{so that } H^s(F) = \begin{cases} \infty & \text{if } s < \dim_H(F) \\ 0 & \text{if } s > \dim_H(F) \end{cases}$$

If $s = \dim_H(F)$, then $H^s(F)$ may be zero, or infinite, or satisfy

$$0 < H^s(F) < \infty$$

Finding the Hausdorff dimension of a set is thus equivalent to finding this critical value for the Hausdorff measure of the set.

4.1.4 The box dimension

Trying to determine the Hausdorff dimension of a set is generally not an easy task, as finding the infimum among all the possible δ -covers of a set is complicated.

Things become easier when we restrict ourselves to sets of diameter δ and of a certain shape. We can define a new dimension, called the box counting dimension, as follows.

Let F be a non-empty bounded set of \mathbb{R}^n , and let $N_\delta(F)$ be the smallest number of subsets of \mathbb{R}^n of diameter δ that cover F . Then we define the lower and upper *box dimension* of F as follows:

$$\underline{dim}_B(F) \equiv \liminf_{\delta \rightarrow 0} \frac{\log(N_\delta(F))}{-\log(\delta)}$$

$$\overline{dim}_B(F) \equiv \limsup_{\delta \rightarrow 0} \frac{\log(N_\delta(F))}{-\log(\delta)}$$

If these two limits are equal, then the *box dimension* of F is

$$dim_B(F) \equiv \lim_{\delta \rightarrow 0} \frac{\log(N_\delta(F))}{-\log(\delta)}$$

We can consider another definition of the box dimension that will make calculations easier, and that we can show to be equivalent to the general definition. Instead of simply considering subsets of \mathbb{R}^n of diameter δ , we will consider a n -dimensional mesh made of cubes of side length δ . This means the cubes will have a diameter $\delta\sqrt{n}$. Let $N'_\delta(F)$ be the number of cubes that intersect F . Then, since the cubes have diameter $\delta\sqrt{n}$,

$$N_{\delta\sqrt{n}}(F) \leq N'_\delta(F)$$

If $\delta\sqrt{n} < 1$,

$$\frac{\log(N_{\delta\sqrt{n}}(F))}{-\log(\delta\sqrt{n})} \leq \frac{\log(N'_\delta(F))}{-\log(\sqrt{n}) - \log(\delta)}$$

and by taking limits as δ tends to 0,

$$\underline{dim}_B(F) = \liminf_{\delta \rightarrow 0} \frac{\log(N'_\delta(F))}{-\log(\delta)}$$

and

$$\overline{dim}_B(F) \leq \limsup_{\delta \rightarrow 0} \frac{\log(N_\delta(F))}{-\log(\delta)}$$

On the other hand, any set of diameter lesser or equal than δ is contained in at most 3^n cubes of the mesh of side δ . This is true because any cube that intersects the set has $3^n - 1$ neighbors, and the set is necessarily fully included in the cube and the neighboring cubes. Thus,

$$N'_\delta(F) \leq 3^n N_\delta(F)$$

By taking the logarithm, dividing both sides by $-\log(\delta)$ and taking the limits when δ tends to 0, we find that

$$\liminf_{\delta \rightarrow 0} \frac{\log(N'_\delta(F))}{-\log(\delta)} \leq \underline{dim}_B(F)$$

and

$$\limsup_{\delta \rightarrow 0} \frac{\log(N_\delta(F))}{-\log(\delta)} = \overline{dim}_B(F)$$

which are the opposite inequalities as those previously found. Thus, we have proven that the definitions of the box dimension taking sets of diameter δ or a mesh of cubes of side δ are equivalent, which is a great asset for calculations.

Moreover, the box dimension has the interesting property that it is equal, for most of the sets that are simple enough, to the Hausdorff dimension. It will be the case for the *Multifractal spectrum* of the financial series we will study in this paper. Thus, we now have a practical way of calculating the Hausdorff dimension of sets.

4.1.5 Example : the dimension of the Cantor Middle Set

In this example, we will calculate both the Hausdorff and the box dimension of the Cantor Middle Set, and will see that they are equal. The set is simple enough so that its Hausdorff dimension can be calculated directly, however as we will see the computation of the box dimension is more straightforward.

Let's formally show that the Hausdorff dimension of the middle Cantor set is $\frac{\log 2}{\log 3}$.

The middle Cantor set F split into a left part F_L and a right part F_R that are similar to F , but scaled by a ratio of $1/3$. Since for all $s \in \mathbb{R}$, H^s is a measure, and since F_L and F_R are disjoint,

$$H^s(F) = H^s(F_L) + H^s(F_R) = \frac{1}{3^s}H^s(F) + \frac{1}{3^s}H^s(F)$$

Assuming that for $s = \dim_H(F)$, $0 < H^s(F) < \infty$, we can divide each side of the previous equality by $H^s(F)$, and obtain that $1 = 2(\frac{1}{3^s})$, thus $\dim_H(F) = \frac{\log 2}{\log 3}$

Now, let's calculate the box dimension of this set. In 1 dimension, n-dimensional cubes are segments. If we partition $[0,1]$ in 3^k segments of length 3^{-k} , the set E_k is covered by 2^k of those segments. Thus, $N'_\delta(E_k) = 2^k$ for $\delta = 3^{-k}$, so

$$\dim_B(F) \leq \limsup_{k \rightarrow \infty} \dim_B(E_k) = \limsup_{k \rightarrow \infty} \frac{\log(2^k)}{\log(3^k)} = \frac{\log 2}{\log 3}$$

and

$$\dim_B(F) \geq \liminf_{k \rightarrow \infty} \dim_B(E_k) = \liminf_{k \rightarrow \infty} \frac{\log(2^k)}{\log(3^k)} = \frac{\log 2}{\log 3}$$

Thus $\dim_B(F) = \frac{\log 2}{\log 3}$, and we have shown that for the Cantor Middle Set, Hausdorff and box dimensions are equal.

4.2 Multifractal Measures

Multifractal measures are built on fractal sets such as the middle Cantor set or the von Koch curve. In this paragraph and in the rest of this paper, we will consider one of the simplest multifractal measures, the *binomial measure* on $[0,1]$. This binomial measure is derived as the limit of a random multiplicative cascade.

4.2.1 The conservative and the canonical binomial measure

Let's consider the uniform probability measure μ_0 on the interval $[0,1]$, and two positive real number m_0 and m_1 such that $m_0 + m_1 = 1$. We built the cascade step by step. At the first step, we define a measure μ_1 on the σ -algebra $\{\emptyset, [0, 1], [0, \frac{1}{2}], [\frac{1}{2}, 1]\}$, such that $\mu_1[0, \frac{1}{2}] = m_0$ and $\mu_1[\frac{1}{2}, 1] = m_1$. Thus, we have allocated a mass m_0 to the left interval and m_1 to the right interval.

In the second step, we split again each one of the subintervals into two, and define a measure μ_2 that allocates a fraction m_0 of the mass of the previous interval to the newly created left-subinterval, and m_1 to the newly created right-subinterval. Thus, we have

$$\begin{aligned} \mu_2[0, \frac{1}{4}] &= m_0 m_0, & \mu_2[\frac{1}{4}, \frac{1}{2}] &= m_0 m_1 \\ \mu_2[\frac{1}{2}, \frac{3}{4}] &= m_1 m_0, & \mu_2[\frac{3}{4}, 1] &= m_1 m_1 \end{aligned}$$

At each step k , we define a measure μ_k , and this sequence of measure weakly converges towards the binomial measure μ .

Consider $t \in [0,1]$ such that t is a dyadic rational number, i.e. there is a finite number of integers $\eta_1, \eta_2, \dots, \eta_k \in \{0, 1\}$ such that $t = \sum_{i=1}^k \eta_i 2^{-i}$. Then, if we denote ϕ_0 the frequency of 0s in its expansion, and ϕ_1 the frequency of 1s, then

$$\mu[t, t + 2^{-k}] = m_0^{k\phi_0} m_1^{k\phi_1}$$

As, at each step, the fractions of the mass allocated to the left and right subinterval sums to 1, the measure is said to be *conservative*.

We can also draw the mass we allocate to each subinterval randomly from a given distribution. At each stage, the mass of the left and right subintervals obtained by multiplying the previous mass by a multiplier M_0, M_1 . We will assume that all the multipliers we will draw have identical distribution M , that M_0 and M_1 are independent, and that they are independent at each step of the construction. When the mass is conserved in average, i.e $(E)(M) = \frac{1}{2}$ or equivalently $\mathbb{E}(M_0 + M_1) = 1$, we say that the measure is *canonical*.

4.2.2 Moment-scaling properties

Multiplicative measures like the binomial measure display moment-scaling properties, meaning that their moments verify a certain relationship with the considered time-scale δt .

For a cell starting at a dyadic rational number $t \in [0,1]$ and of length 2^{-k} , $\mu(\Delta t)$ is equal to the product of the multipliers allocated to the dyadic intervals in which the cell belongs. For a *conservative* measure, if $t = \sum_{i=1}^k \eta_i 2^{-i}$, then $\mu(\Delta t) = M_{\eta_1} M_{\eta_1 \eta_2} \dots M_{\eta_1 \eta_2 \dots \eta_k}$. Since we considered the multipliers to be independent at each stage of refinement of the measure μ_k , for any $q \in \mathbb{R}^+$, $\mathbb{E}[\mu(\Delta t)^q] = [\mathbb{E}(M^q)]^k$. So we can write:

$$\mathbb{E}[\mu(\Delta t)^q] = (\Delta t)^{\tau(q)+1}$$

where τ is called the *scaling function* and

$$\tau(q) = -\log_b \mathbb{E}(M^q) - 1$$

For a *canonical* measure, we have to consider that the measure of interval $[0,1]$ itself is a random variable, that we will denote $\Omega = \mu[0,1] \geq 0$. Then $\mu(\Delta t) = M_{\eta_1} M_{\eta_1 \eta_2} \dots M_{\eta_1 \eta_2 \dots \eta_k} \Omega$. Thus, for a canonical measure the scaling relationship is:

$$\mathbb{E}[\mu(\Delta t)^q] = \mathbb{E}(\Omega^q) (\Delta t)^{\tau(q)+1}$$

4.2.3 Definition

A random measure μ defined on $[0,1]$ is a *multifractal measure* if, for all $q \in \mathbb{Q}$:

$$\mathbb{E}(\mu[t, t + \Delta t]^q) \sim c(q) (\Delta t)^{\tau(q)+1} \text{ as } \Delta t \rightarrow 0$$

and where \mathbb{Q} is an interval containing $[0,1]$, and τ and c are deterministic functions defined on \mathbb{Q} . Note that the binomial measure we have defined previously is a grid-bound construction: it verifies the definition only on a certain grid (t must be a dyadic rational number). However, we will see with the continuous MSM that grid-free models also exist.

4.3 The Multifractal formalism

In the following subparts, we will use the notions previously presented to introduce the use of multifractals to study financial series. As it has been previously suggested, the fractal properties of the financial series lie in their statistical behavior.

As we will see later in this paper, the log-returns of a security can be represented by a special kind of stochastic process, a *multifractal process*. These multifractal processes are built by compounding well known processes such as Brownian motions, with the cumulative distribution function of a multifractal measure such as the binomial measure. Inversely, if we assume the log-normal returns follow such a law, then the properties of the multifractals will help us identify the various underlying parameters of the model, such as the distribution M used when building the binomial measure. In this part, we will define the multifractal spectrum of a process, and see how it relates to its scaling function.

4.3.1 Local Hölder Exponent

First, we will define the Local Hölder exponent of a function : given $t \in \mathbb{R}^{*+}$, let g be a function defined in the neighborhood of t . Then the number

$$\alpha(t) = \sup\{\beta : |g(t + \Delta t) - g(t)| = \mathcal{O}(|\Delta t|^\beta) \text{ as } \Delta t \rightarrow 0 \text{ and } \beta \geq 0\}$$

is called the Hölder exponent of g at t .

This Local Hölder exponent measures the regularity of the function g at t . Heuristically, around t , $|dg| \approx (dt)^{\alpha(t)}$. Thus, the lower $\alpha(t)$ is, the more irregular g is at t . If g is bounded around t , then $\alpha(t) \geq 0$. For a classical Brownian motion, $\alpha(t) = 1/2$ along the path.

4.3.2 Fractional Brownian Motion

We take this opportunity to define the *Fractional Brownian Motion*, which is a stochastic process verifying the same assumptions of stationary and Gaussian increments, continuity and initial condition than the classic Brownian Motion, to the exception that the increments may not be independent anymore. For any real number H between 0 and 1, $t > s > 0$, the covariance of the Fractional Brownian Motion B_H verifies:

$$\mathbb{E}[B_H(t)B_H(s)] = \frac{1}{2}(t^{2H} + s^{2H} - (t - s)^{2H})$$

For a classic Brownian Motion, $H=1/2$ so $\mathbb{E}[B_H(t)B_H(s)] = s$. For any Fractional Brownian Motion, the Local Hölder exponent is equal to H along the path. If $H > 1/2$, the returns are positively correlated and B_H has a higher regularity than a Brownian Motion. If $H < 1/2$, the returns are negatively correlated, and B_H is less regular than a classic Brownian motion.

4.3.3 The Multifractal Spectrum

The Local Hölder exponent can vary a lot in function of t for a multifractal process. Thus, it appears more interesting to study the distribution of $\alpha(t)$ at random instants. To do so, we first note that

$$\alpha(t) = \liminf_{\Delta t \rightarrow 0} \frac{\ln|g(t, \Delta t)|}{\ln(\Delta t)}$$

where $g(t, \Delta t) \equiv g(t + \Delta t) - g(t)$.

For $k \geq 1, b \in \mathbb{N}^*$, we divide the unit interval into b^k subintervals of length $\Delta t = b^{-k}$. For each interval, we can calculate the *coarse* Hölder exponent

$$\alpha_k(t_i) \equiv \frac{\ln|g(t_i, \Delta t)|}{\ln(\Delta t)}$$

which generates b^k observations of the Hölder exponent.

We afterwards divide the range of α s into small ranges $[\alpha, \alpha + \Delta\alpha]$ of length $\Delta\alpha$, and we define $N_k(\alpha)$, the number of observations in the interval $[\alpha, \alpha + \Delta\alpha]$.

This allows us to define the *Multifractal Spectrum* :

$$f(\alpha) = \lim \left(\frac{\ln(N_k(\alpha))}{\ln(b^k)} \right) \text{ as } k \rightarrow \infty$$

The Multifractal spectrum is an extremely important notion in the domain of multifractal measures, especially when combined with the identity below that links it to a process' scaling function. The steps that we have taken just before, by cutting both the the time and the range of α s in intervals, thus creating boxes, reminds us of the ways used to calculate the Hausdorff dimension of a set in practice. In fact, this is exactly what we have done: for a given process g and a given α , $f(\alpha)$ is the Hausdorff dimension of the set of instants t for which α is the local Hölder exponent of g at t .

For Multifractal measures, a fundamental identity relates the multifractal spectrum of the measure to their scaling function:

$$f(\alpha) = \inf_q [\alpha q - \tau(q)]$$

We say that $f(\alpha)$ is the *Legendre transform* of the scaling function $\tau(q)$.

This identity is fundamental, since it will allow us to identify parameters used to build a Random multiplicative cascade. As we will see in the study of Continuous MSM model, the previous identity can help us determine the distribution M of the mass allocation at each step of the construction of the binomial measure.

Assume we are studying a process, such as a financial series. As we will see in the next part dedicated to Multifractal processes, an asymptotic study of the moments q of the returns when their lag tends to 0 allows us to determine the scaling function of the log-returns. From the knowledge of the scaling function, the previous identity allows us to deduce the multifractal spectrum of the log-returns.

Depending on the shape of the graph of the multifractal spectrum, the law of $-\log_2(M)$ can be deduced (and thus, the law of M). For instance, if f is parabolic, this indicates that M follows a log-normal distribution, such that $-\log_2(M) \sim \mathcal{N}(\lambda, \sigma^2)$ where λ and σ are parameters to be determined. From the condition that for a canonical measure $\mathbb{E}(M) = 1/2$, we obtain the relationship : $\sigma^2 = 2(\lambda - 1)/(\ln 2)$. Since $\tau(q) = -\log_2(M) - 1$, we can easily show that $\tau(q) = \lambda q - 1 - q^2 \sigma^2 (\ln 2)/2$. We obtain the multifractal spectrum by taking the Legendre transform of the scaling function:

$$f_\theta(\alpha) = 1 - \frac{(\alpha - \lambda)^2}{4(\lambda - 1)}$$

By identifying the maximum of f 's curve, we can obtain λ , and thus σ .

Thus, if we assume a process is a multifractal process (motivated by Economic considerations), this framework will help us identify its main features and therefore calibrate our model for future forecasting.

4.4 Multifractal processes

We say that a stochastic process $X(t)$ is a *Multifractal process* if it has stationary increments and if for every $q \in \mathbb{R}^{*+}$, it satisfies the moment scaling rule:

$$\mathbb{E}(|X(t + \Delta t) - X(t)|^q) \sim c_X(q)(\Delta t)^{\tau_X(q)+1}$$

We say that a process is *self-similar* if its scaling function $\tau_X(q)$ is linear. Since $\tau_X(0) = -1$, if we call H the slope of the scaling function, then:

$$\tau_X(q) = Hq - 1$$

Thus, the scaling function of a self-similar process is fully determined by its slope H . We call these processes *unifractal*. The notation H for the slope is not random: it reminds us of the Fractional Brownian Motion, and rightly so. Indeed, for a Fractional Brownian motion B_H , $t > 0$, $\Delta t > 0$, we have that $|B_H(t + \Delta t) - B_H(t)|^q = B_H(1)^q (t - s)^H q$. Thus, $\tau_{B_H}(q) = Hq - 1$.

We will use this property when we will study the Multifractal Model of Asset Returns and the Continuous MSM, where we will model the log-returns of financial series by a Fractional Brownian Motion compounded with the cumulative distribution function of a multifractal measure.

5 Multifractal Models

5.1 The Markov-Switching Multifractal in Discrete Time (MSM)

5.1.1 Model presentation

The Markov-Switching Multifractal model follows the intuition that the returns of the market are impacted by economic uncertainties that have various degrees of persistence and occurrence.

The MSM volatility is the product of a finite number of components, which are random-first order Markov processes. These components are identical except in their regime switching probabilities, which grow geometrically with the index of the component

We consider a series P_t of the prices of an asset, defined in discrete time over a regular time grid $t=0,1,\dots,\infty$. $r_t = \ln(P_t/P_{t-1})$ denotes the log-returns. We define \bar{k} Markov components that drive the volatility, forming the vector

$$M_t = (M_{1,t}; M_{2,t}; \dots; M_{\bar{k},t}) \in \mathbb{R}_+^{\bar{k}}$$

The dynamics of the Markov components is the following. Assume the vector has been constructed until date $t-1$, each component $M_{k,t}$ $k \in 1, \dots, \bar{k}$ is drawn from the same, fixed distribution M , with probability γ_k , or is left unchanged and equal to its previous value $M_{k,t} = M_{k,t-1}$.

To summarize,

$M_{k,t}$ is drawn from distribution M with probability γ_k

$$M_{k,t} = M_{k,t-1} \text{ with probability } 1 - \gamma_k$$

with independent switching events across k and t . We require that M has positive support and unit mean: $M \geq 0$ and $\mathbb{E}(M) = 1$

Thus, the components of M_t have the same marginal distribution but evolve with different frequencies. Indeed, the multipliers differ only in their transition probabilities γ_k . The multipliers are nonnegative, and satisfy $M_{k,t} \geq 0$ and $\mathbb{E}(M_{k,t}) = 1$ for all t and k . Moreover, the components of different frequencies are mutually independent : $M_{k,t}$ and $M_{k',t'}$ are independent for every t and t' if $k \neq k'$.

From the Markov multipliers, we model the stochastic volatility as follows :

$$\sigma(M_t) = \bar{\sigma} \left(\prod_{k=1}^{\bar{k}} M_{k,t} \right)^{1/2}$$

where $\bar{\sigma}$ is a positive constant parameter. The returns are then modeled as follows :

$$r_t = \sigma(M_t) \epsilon_t$$

where ϵ_t are i.i.d. standard Gaussian variables $\mathcal{N}(0,1)$.

The transition probabilities are defined as follows

$$\gamma_k = 1 - (1 - \gamma_1)^{b^{k-1}}$$

where $\gamma_1 \in (0,1)$ and $b \in (0,\infty)$. For small values of γ_1 and b , the transition probability grows geometrically with k :

$$\gamma_k \approx \gamma_1 b^{k-1}$$

For low-frequency components, the transition probabilities grow approximatively a geometric rate b .

For simplicity, we will assume a binomial distribution for the random variable M , which can only take two values, m_0 or m_1 . These outcomes will have equal probability, and verify $m_1 = 2 - m_0$.

$MSM(\bar{k})$, the MSM model with \bar{k} frequencies, allows a description of volatility with a potentially high number of components at a low cost. In a general Markov Chain, one would need to know a transition matrix to be able to compute $M_{t,k}$ knowing $M_{t-1,k}$, and this transition matrix would have $2^{2\bar{k}}$ elements. As usually 10 components are used to perform these simulations, this would imply having a model with more than a million parameters. The binomial MSM is parsimonious since it requires only four parameters. The full parameter vector is

$$\psi \equiv (m_0, \bar{\sigma}, b, \gamma_{\bar{k}}) \in \mathbb{R}_+^4$$

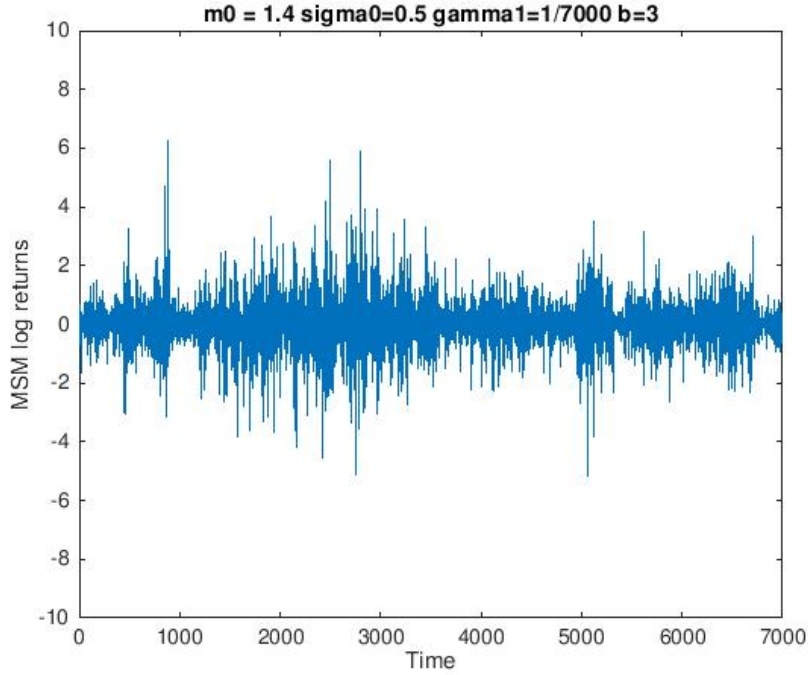


Figure 5: Illustrations of the simulated log-returns with the binomial Markov switching model. The process has $\bar{k} = 7$ frequencies, and the parameters are $m_0 = 1.4$, $\sigma_0 = 0.5$, $\gamma_1 = 1/7000$, and $b = 3$

5.1.2 Stylized properties

We simulated returns with the MSM model using $\bar{k} = 7$ frequencies, by choosing $m_0 = 1.4$, $\sigma_0 = 0.5$, $\gamma_1 = 1/7000$ and $b = 3$. We represented these returns in function of time in Figure 5.

As we can observe in Figure 5, there is both a volatility clustering and a heterogeneity in volatility levels. Indeed, periods with high volatility in returns alternate with periods with lower volatility, but these periods also tend to persist. This indicates that during these periods, many of the first components (with a low probability of switching) take either a high or a low value, and thus high or low level of volatility persist.

Moreover, the returns display a long memory feature. It is defined by a hyperbolic decline in the autocorrelation function as the lag goes to infinity. Thus if we define:

$$\rho_q(n) = \text{Corr}(|r_t|^q, |r_{t+n}|^q) \text{ for } q \geq 0 \text{ and } n \in \mathbb{N}$$

$\rho_q(n)$ will slowly decline with n , the lag. A hyperbolic decline means that, contrary to an exponential decline for which the autocorrelation rapidly tends to 0 when the lag grows, the autocorrelation still remains significantly positive with higher values of n and decreases more slowly. This is why we say that the process displays a Long memory feature. In Figure 6 we have represented the decline in autocorrelations of the second moments of the returns in function of the lag by performing a Monte-Carlo simulation over 300 paths. Each path has been simulated over 10000 time-steps, and the parameters of the Discrete MSM are identical to those used before : $\bar{k} = 7$ frequencies, $m_0 = 1.4$, $\sigma_0 = 0.5$, $\gamma_1 = 1/7000$, and $b = 3$.

It can be shown formally that for small values of n , the decline is hyperbolic, which means that there exist a positive function δ of q such that

$$\log(\rho_q(n)) \approx -\delta(q)\log(n)$$

and that for n sufficiently large, the autocorrelation transitions to an exponential decline, meaning that there exists a positive function α of q such that

$$\log(\rho_q(n)) \approx -\alpha(q)n$$

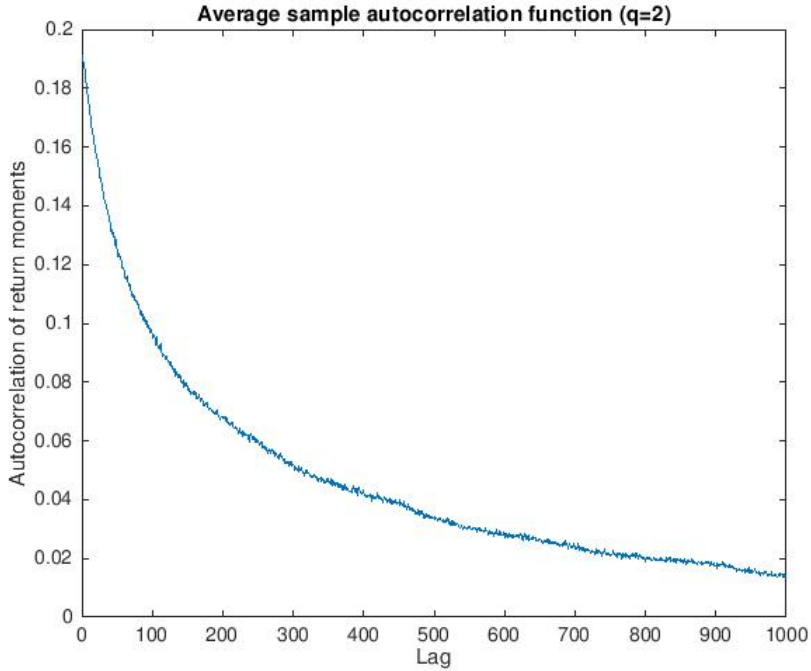


Figure 6: Graph of the autocorrelation of the second moment of log-returns ($q=2$) simulated with the binomial Markov switching model. The process has $\bar{k} = 7$ frequencies, and the parameters are $m_0 = 1.4$, $\sigma_0 = 0.5$, $\gamma_1 = 1/7000$, and $b = 3$. The graph has been obtained by doing a Monte-Carlo simulation over 300 paths, each having 10000 time steps.

In Figure 7, we represented the logarithm of the autocorrelation of the second moment of the returns in function of the logarithm of the lag. We can observe that for small values of n ($n \leq 8$), the curve has a constant negative slope, which testifies of the hyperbolic decline.

In Figure 8, we represented this time the logarithm of the autocorrelation of the second moment of the returns in function of the lag, and observe that for higher values of n ($n > 500$), the curve has a constant negative slope, which testifies of the exponential decline for higher values of n .

We can also plot a histogram of the returns obtained with these models, and observe that the tails are thicker than the tails for a normal distribution of the returns (see Figure 9). Indeed since the volatility varies over time, it reaches levels that are higher than σ_0 and sticks to these high levels for a certain period of time because of the slow decline in autocorrelations. Thus, extreme returns are more common than with a normal distribution of returns.

5.2 The Multifractal Model of Asset Returns (MMAR)

5.2.1 Model presentation

The key idea behind multifractal diffusion models such as the MMAR or the Continuous-Time MSM is the compounding of a Brownian Motion with a multifractal time deformation. These models exhibit the property of moment-scaling: the moments of the returns scale as a power-law of the frequency of observation.

In the MMAR, the multifractal time deformation is the cumulative distribution function of a random multiplicative cascade. The models exhibits properties such as moment-scaling, thick tails and long memory volatility persistence, which are observed empirically in financial series. Moreover, the MMAR is a diffusion model outside of the class of classic Itô diffusions: while the sample paths of Itô diffusions vary locally as $(dt)^{1/2}$, the MMAR paths can vary as $(dt)^{\alpha(t)}$ where $\alpha(t)$ takes a continuum of values on any finite interval.

Let's note $P(t)$ the price of a financial asset at time t , for t in a bounded interval $[0, T]$. We define the log-price process:

$$X(t) \equiv \ln P(t) - \ln P(0)$$

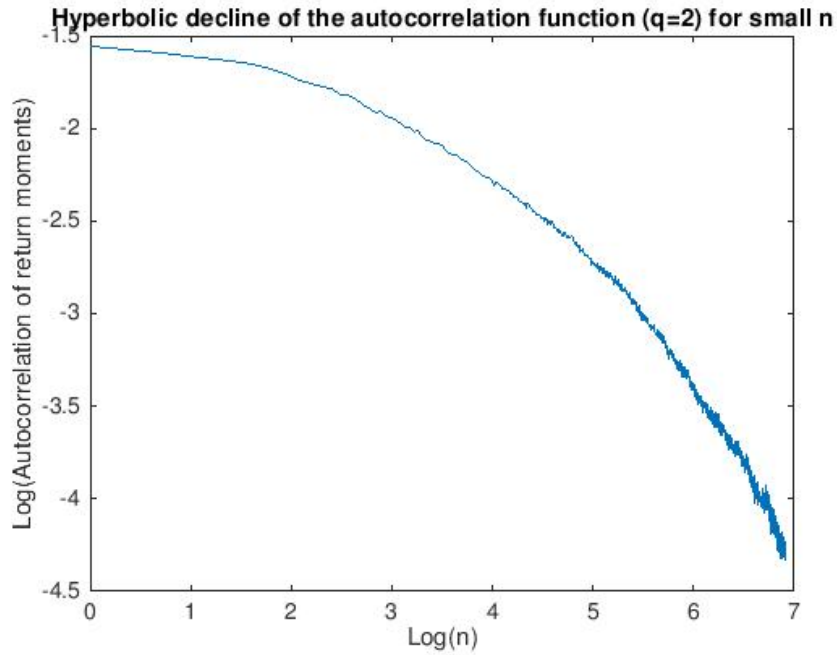


Figure 7: Graph of the logarithm of the autocorrelation of the second moment of log-returns ($q=2$) in function of the logarithm of the lag. As for $n \leq 8$ the graph has a constant slope, this illustrates a hyperbolic decline in the autocorrelation of the moment of the returns for small values of n .

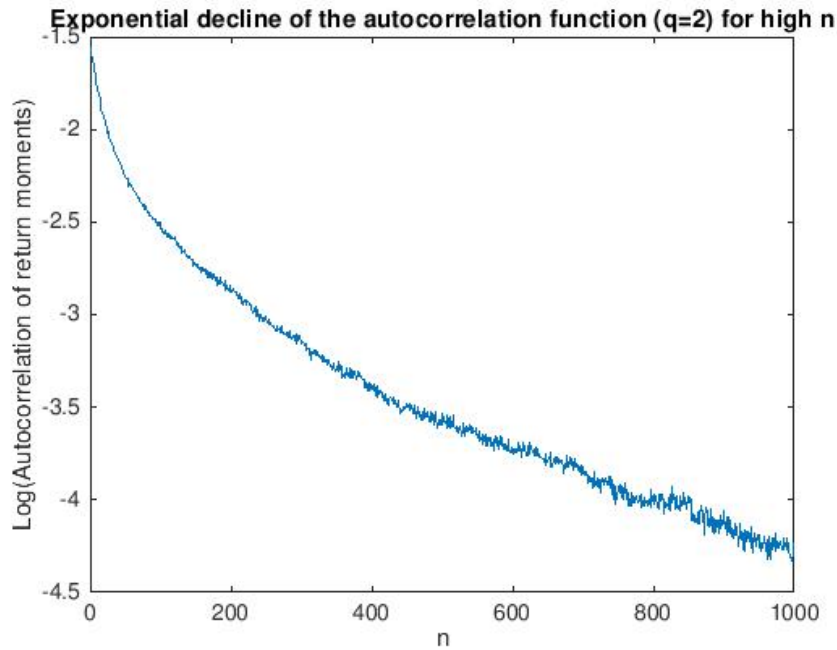


Figure 8: Graph of the logarithm of the autocorrelation of the second moment of log-returns ($q=2$) in function of the lag. As for $n \leq 8$ the graph has a constant slope, this illustrates an exponential decline in the autocorrelation of the moment of the returns for high values of n .

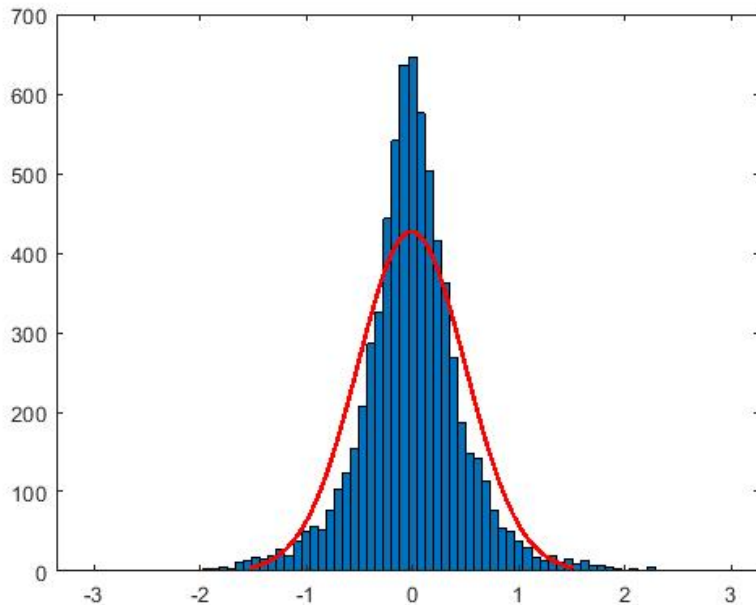


Figure 9: Distribution of the returns obtained with the Discrete MSM model, fitted by a normal distribution of the returns. We observe the tails are thicker for our model, because the volatility is not constant..

The MMAR is built by imposing three conditions on the log-price $X(t)$:

Condition 1: $X(t)$ is a compound process

$$X(t) \equiv B[\theta(t)]$$

where $B(t)$ is a Brownian motion and $\theta(t)$ is a stochastic time deformation

Condition 2: The stochastic time deformation $\theta(t)$ is the cumulative distribution function of a multifractal measure, which is a random multiplicative cascade μ defined on $[0, T]$, that is $\theta(t) = \mu[0, t]$

Condition 3: The processes $B(t)$ and $\theta(t)$ are independent

Under these conditions, the moments of the log-price are given by:

$$\mathbb{E}[|X(t)|^q] = \mathbb{E}[\theta(t)^{q/2}] \mathbb{E}[|B(1)|^q]$$

and since $\mathbb{E}[\theta(t)^q] \sim c_\theta(q)t^{\tau_\theta(q)+1}$, therefore

$$\mathbb{E}[|X(t)|^q] \sim c_X(q)t^{\tau_X(q)+1} \text{ as } t \rightarrow 0$$

where $\tau_X(q) = \tau_\theta(q/2)$ and $c_X(q) = c_\theta(q/2)\mathbb{E}[|B(1)|^q]$. This means that the moments of the returns scale as a power function of the frequency of observation. We recognize here the definition of a multifractal process : the log-price produced by the MMAR is indeed a multifractal process.

5.2.2 Building a MMAR simulation

We will illustrate how to simulate MMAR returns. Since in the MMAR, the log-price process is a Brownian motion compounded with a time-deformation $\theta(t)$, we first need to build this deformation.

$\theta(t)$ is the cumulative distribution function of a multifractal measure, which is a multiplicative cascade. This measure can be conservative or canonical. We will construct two MMAR simulations : one based on a conservative measure, and one based on a canonical measure. In both cases, the measure is binomial, so the interval $[0, T]$ is cut into dyadic intervals. Here for simplification, we considered $T=1$. In order to build the measures in practice, we have to restrict ourselves to a finite number of intervals, which is here equal to $2^{10} = 1024$. The fact that the MMAR is built in practice on this dyadic intervals is also one of its main drawbacks: we say that the MMAR is

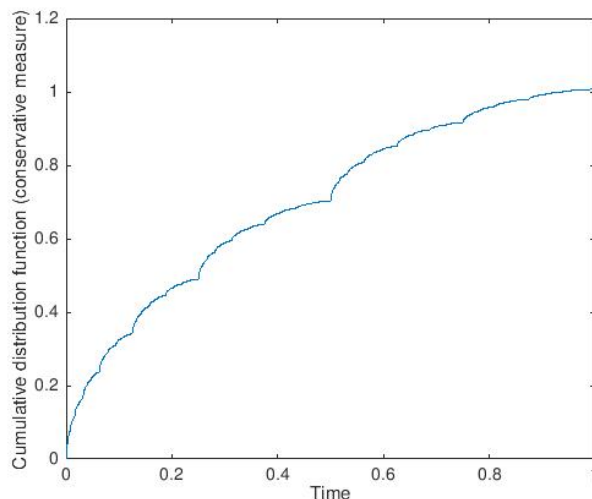


Figure 10: Cumulative distribution function of a conservative measure (multiplicative cascade). We chose $m_0 = 1.4$ and $m_1 = 2 - m_0 = 0.6$.

built on a grid. This implies that the MMAR is a non-stationary process, a drawback that will be tackled by the Continuous MSM model.

Figure 10 illustrates the cumulative distribution function of a conservative measure, for which we have chosen the distribution M to be discrete and take only two values m_0 or m_1 such that $m_0 + m_1 = 2$. As we can observe, the c.d.f. grows regularly, and $\mu[0, 1] = 1$, which is characteristic of a conservative measure. Moreover, some particular points are exhibited: the first dyadic was allocated only m_0 masses and we chose $m_0 = 1.4$, thus the measure of the first dyadic interval will be the highest among all the dyadic intervals. Thus, this is the interval on which the c.d.f. will grow the most rapidly, fact that is verified on the graph. Similarly, the measure of the last dyadic interval is the lowest, so this is where the c.d.f. will grow the least. We also observe that just before hitting 0.5, the c.d.f. grows slowly, and very rapidly just after. This is again because the dyadic interval $[0.5, 0.5 - 2^{-10}]$ was only allocated the mass m_0 once in ten allocations, whereas the interval $[0.5 + 2^{-10}, 0.5]$ as only allocated the mass m_1 once in ten allocations.

Figure 11 illustrates the cumulative distribution function of a canonical measure. We have chosen the uniform distribution $M = \mathcal{U}[0, 2]$, which fulfills the conditions $E(M)=1$, necessary for a canonical measure. As we can see, the c.d.f. grows very erratically when compared to Figure 10. In particular, we can see a huge spike around 0.4, which is due to the fact that masses aren't allocated on a "left-right" basis at step like for the conservative measure, but are randomly drawn from $[0, 2]$. Moreover, we observe that $\mu[0, 1] > 1$, which is not abnormal for a canonical measure, contrary to a conservative measure.

After having built the trading time $\theta(t)$, we obtain the log-price $X(t)$ by compounding a Brownian motion with the trading time. We have done so and represented the Price, given by $P_0 e^{X(t)}$ for both the conservative and the canonical measure, respectively in Figure 12 and Figure 13. We have afterwards represented the returns for both measures, respectively in Figure 14 and in Figure 15. As expected from the graphs of our conservative and canonical measures, the returns are smoother for the conservative measure than for the canonical one. Indeed, we observe for the returns obtained with the canonical measure a huge spike in volatility around $t=0.4$, which is the point around which the c.d.f. of the canonical measure brutally grows.

5.2.3 Stylized properties

As it can be seen in Figure 14 and in Figure 15, the MMAR returns display volatility clustering at all time scales, and intermittent large fluctuations in volatility.

As we did previously, we could intend to have a look at the autocorrelation of the moments of returns and see if they decrease hyperbolically. However now, the time range is continuous, and is not defined only discretely as it was in the Discrete MSM model. Thus, we need to define the autocorrelation differently. In the MMAR, it is actually the process $X(t)$, the log-price, that

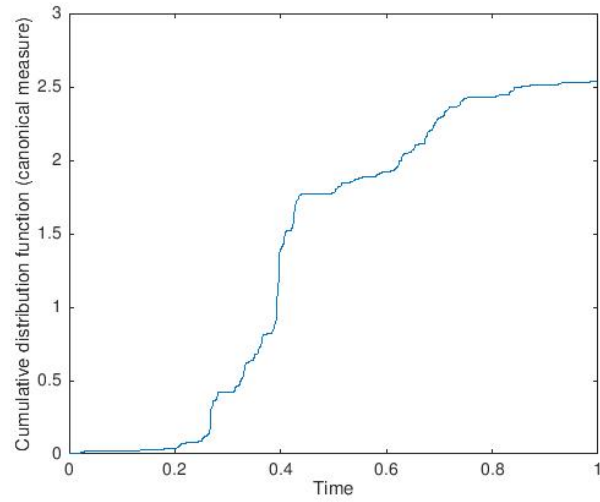


Figure 11: Cumulative distribution function of a canonical measure (random multiplicative cascade). We chose $M = \mathcal{U}[0, 2]$.

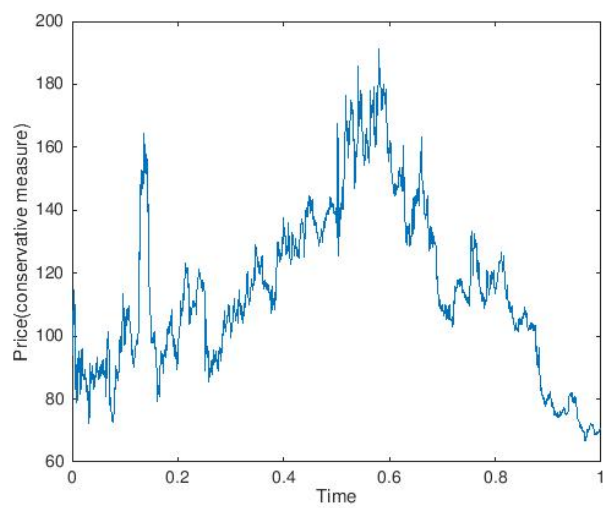


Figure 12: Prices obtained with the MMAR and a conservative measure. $P_0 = 100$

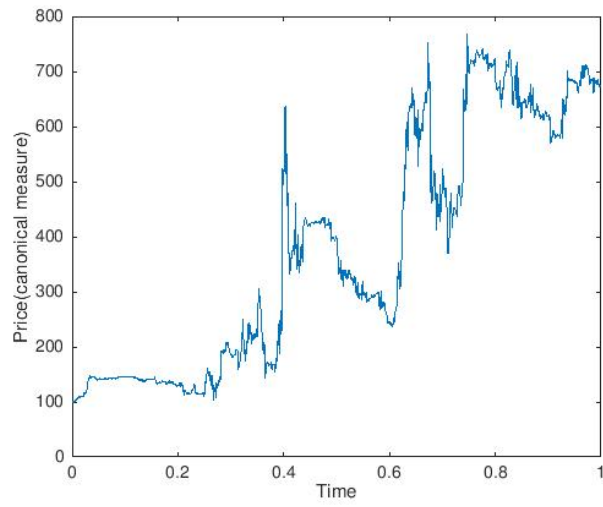


Figure 13: Prices obtained with the MMAR and a canonical measure. $P_0 = 100$

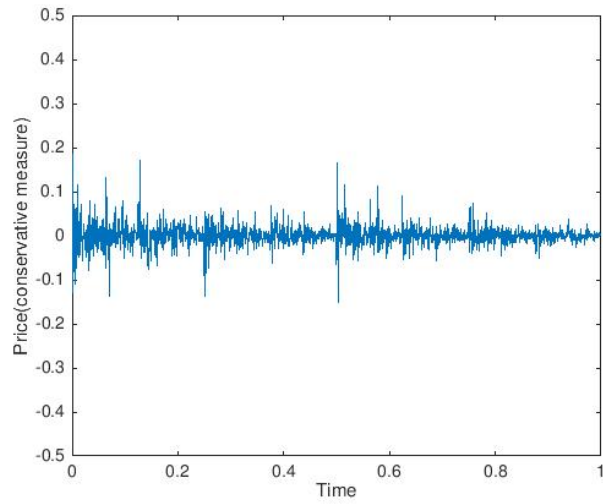


Figure 14: Returns obtained with the MMAR and a conservative measure.

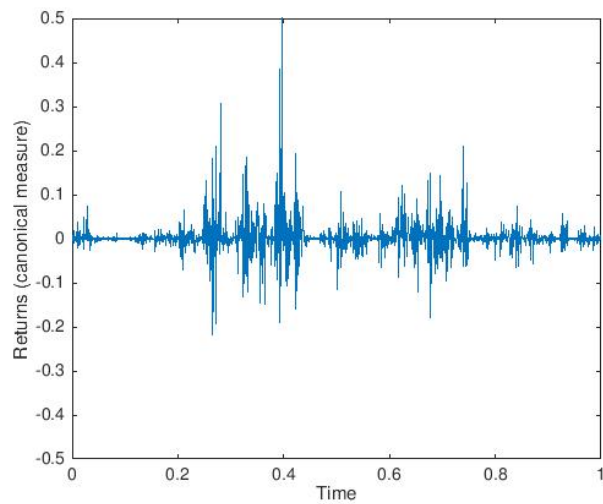


Figure 15: Returns obtained with the MMAR and a canonical measure.

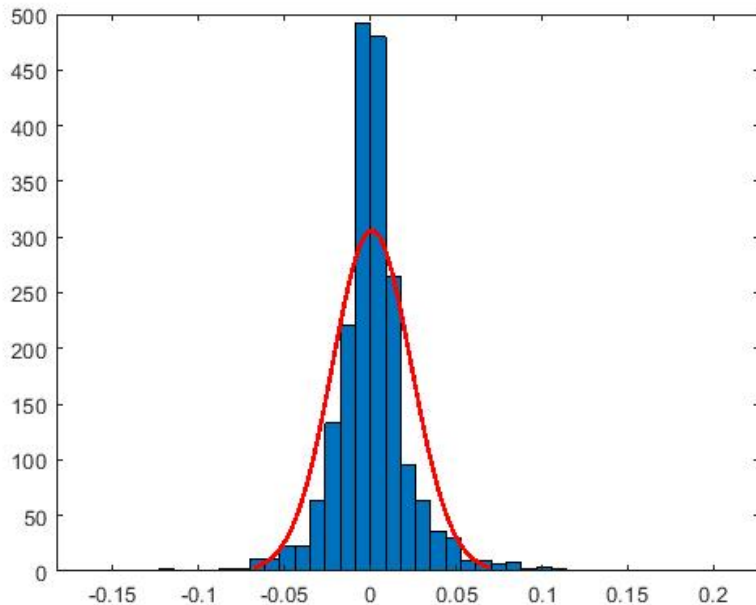


Figure 16: Distribution of the returns obtained with the MMAR model with a conservative measure, fitted by a normal distribution of the returns. We observe the tails are thicker for our model: accelerations and slow-downs in trading time affect the volatility, making it occasionally attain high levels.

displays a Long memory feature. We define the *autocovariance in levels* as follows:

$$\delta_X(t, q) \equiv Cov(|X(a, \Delta t)|^q, |X(a + t, \Delta t)|^q)$$

where $X(a, \Delta t) \equiv X(a + \Delta t) - X(a)$. We say that a process displays a long-memory feature in the size of increments if the autocovariance in levels decreases hyperbolically in t as $t/\Delta t$ tends to ∞ . It can be shown formally that the log-price $X(t)$ displays a long memory feature.

Finally, by observing the distribution of the returns in the model built with a conservative measure compared to a normal distribution of the returns, we see that the tails are again thicker. The trading-time is made of accelerations and slow-downs, which in turn lead the volatility to grow or diminish. For this reason, extreme returns are more common than in a normal distribution, and very small absolute returns are also very common (because periods of low volatility tend to last).

5.3 Continuous-Time MSM

5.3.1 Model presentation

Continuous-Time MSM is built consistently with the discrete time MSM, but allows volatility to have a countable number of components. Moreover, it is an improvement of MMAR since, as we will see, it is defined on an unbounded time range.

Just as for the Discrete-time MSM, Continuous-Time MSM can be built around a finite number $mark$ of Markov components defined as follows:

$$M_t = (M_{k,t})_{k=1,\dots,\infty} \in \mathbb{R}_+^\infty$$

The dynamics of the components are this time triggered by Poisson arrivals, with intensity γ_k for component k .

$M_{k,t}$ is drawn from distribution M with probability $\gamma_k dt$

$$M_{k,t} = M_{k,t-1} \text{ with probability } 1 - \gamma_k dt$$

The Poisson arrivals are independent across k and t , and the distribution M verifies $M \geq 0$ and $\mathbb{E}(M) = 1$.

The arrivals intensities follow a geometric progression:

$$\gamma_k = \gamma_1 b^{k-1}, k \in 1, \dots, \bar{k}$$

b is the base of the multifractal generating process. We will commonly use $b=2$.

The log-price is defined as:

$$X(t) \equiv \ln P(t) - \ln P(0)$$

and has a stochastic volatility :

$$\sigma(M_t) = \bar{\sigma} \left(\prod_{k=1}^{\bar{k}} M_{k,t} \right)^{1/2}$$

where $\bar{\sigma}$ is a positive constant. The process $X(t)$ also has a constant drift \bar{g} , and is then defined as :

$$X(t) = \bar{g}t + \int_0^t \sigma(M_s) dZ(s)$$

where Z is a standard Brownian motion.

Similarly to the discrete-time MSM, the Continuous Time MSM model is fully specified by a vector of four parameters $(\bar{g}, \bar{\sigma}, b, \gamma_1) \in \mathbb{R}_+^4$ and by a distribution M .

MSM can also be defined with countably many components. We consider these components $M_t = (M_{k,t})_{k=1, \dots, \infty} \in \mathbb{R}_+^\infty$, with dynamics driven by Poisson arrivals with intensities $\gamma_k = \gamma_1 b^{k-1}$ and a fixed distribution M . However this time, instead of building a volatility by taking the product of the Markov components, we will consider the time-deformation :

$$\theta_{\bar{k}}(t) \equiv \int_0^t \sigma_{\bar{k}}^2(M_s) dx$$

It can be shown that $\theta_{\bar{k}}(t)$ converges weakly towards a limit distribution $\theta_\infty(t)$ for all t . We will call this limit distribution the trading-time. Then it can be shown that the q^{th} moment of the trading time verifies:

$$\mathbb{E}[|\theta_\infty(t)^q|] \sim c_q t^{\tau_\theta(q)+1} \text{ as } t \rightarrow 0$$

In the Continuous-Time MSM with countably many components, we will represent the log returns $X(t)$ by

$$X(t) \equiv \bar{g}t + B[\theta_\infty(t)]$$

with the processes $B(t)$ and $\theta_\infty(t)$ being independent. The log-returns then satisfy the asymptotic moment scaling property :

$$\mathbb{E}[|X(t)|^q] \sim C_q t^{\tau_X(q)+1} \text{ as } t \rightarrow 0$$

As an extension, we can also model the log-returns by

$$X(t) \equiv \bar{g}t + B_H[\theta_\infty(t)]$$

where $B_H(t)$ and $\theta_\infty(t)$ are independent processes. $H=1/2$ leads to a standard Brownian motion, whereas $H < 1/2$ leads to anti-persistent log-returns X , with much less regularity than a standard Brownian motion. With $H > 1/2$, the log-returns show positive auto-correlations and long-memory.

The Continuous-Time MSM with Countably Many frequencies is thus characterized by the parameters $\bar{\sigma}, \gamma_1$ and b , the distribution M , and if necessary by the Hurst index H . Alternatively instead of looking for the parameters, we can calibrate the model by finding the distribution of the limit time deformation θ_∞ , which is what we will do later.

5.3.2 Building a Continuous MSM simulation

The main difference in the construction of the Continuous MSM simulation in comparison with the one in Discrete time is that now, the arrivals for the different components happen at random moments.

For each $k \in 1, \dots, \bar{k}$, an arrival takes place between t and $t+dt$ with a probability $\gamma_k dt$ (see Paragraph 5.3.1). The time of the arrival must here be randomly drawn, in function of the probability γ_k . The interval Δt_k between two arrivals for the component k follows the law:

$$\Delta t_k \sim \frac{-\log(\mathbb{U}[0, 1])}{\gamma_k}$$

This allows us to find the arrival times for every component, and therefore to simulate the values taken by the components at every point in time by drawing from the distribution M at every arrival. We have done so for the first, the fourth and the tenth Markov component of volatility and represented them in Figures 17, 18 and 19. Again, we see that the higher k is, the more frequent the arrivals are. Also in this model, unlike in the Discrete MSM that we previously simulated, we recall that the distribution M is not a simple binary distribution, but that it is lognormal.

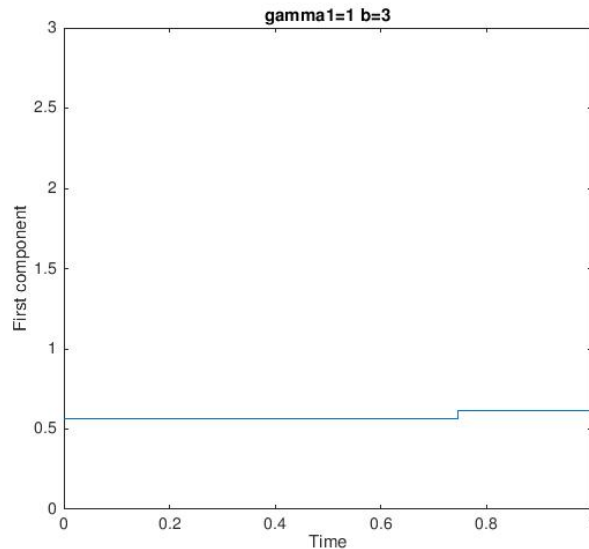


Figure 17: First Markov component in continuous time.

By multiplying the components we have simulated, we obtain the volatility in the case of the Continuous-Time MSM with finitely many components (ten components). As we can see in Figure 20, the volatility tends to cluster at different levels, which is characteristic of Multifractal models.

We can therefore simulate the returns of the Continuous-MSM with finitely (10) many components similarly as we did before, see Figure 21.

To simulate the MSM with countably many components, we first need to obtain the trading time $\theta_\infty(t)$. This trading time is in the form of a limit, and we will take $k=12$ components, for the simulation see 5.3.1. Our trading-time is plotted on Figure 22.

Finally, by compounding the a standard Brownian motion with the trading time previously obtained, we can simulate the log price process $X(t)$ (see Figure 23).

5.3.3 Stylized properties

As we can observe both for the Continuous Time MSM with finitely many components (Figure 21) and with countably many components (Figure 23), these models allow volatility to cluster.

To verify that the multifractal properties of the model hold, we have to check the moment scaling properties of the trading time $\theta(t)$ and of the log-price. In Figure 24, we observe the linearity of the plots for which the slope is theoretically equal to $\tau_\theta(q)$, the scaling function of the trading time. In Figure 25, we observe this time the linearity of the plots for which the slope is

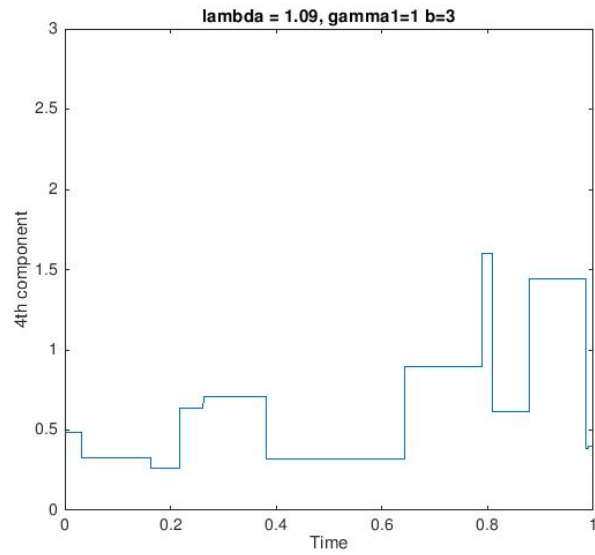


Figure 18: Fourth Markov component in continuous time.

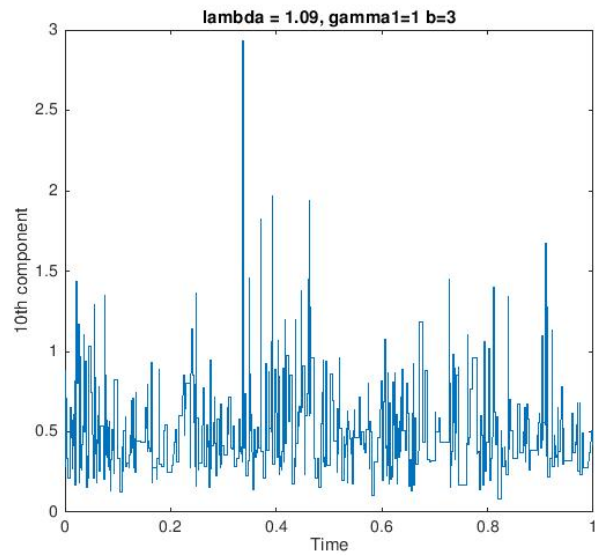


Figure 19: Tenth Markov component in continuous time.

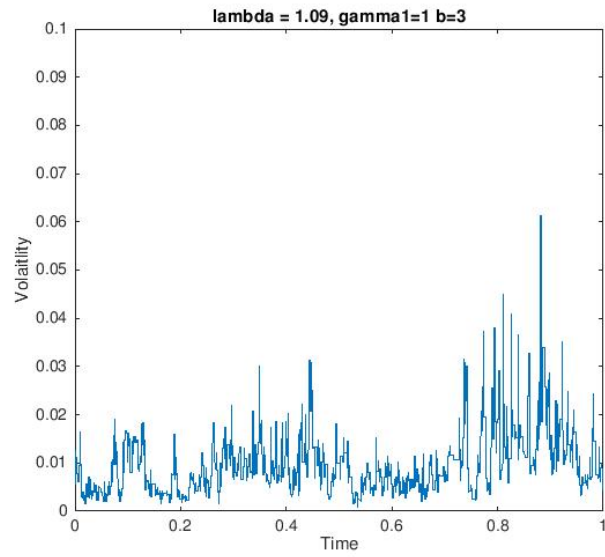


Figure 20: Volatility obtained by multiplying the square root of the Markov components. We have chosen $\sigma_0 = 0.5$, and $k=10$ Markov components.

theoretically equal to $\tau_X(q)$, the scaling function of the log-price process. Both these properties hold well, thus the theory is verified by our simulations.

Similarly as for the MMAR we have a distribution of the returns with thicker tails than the one implied by a normal distribution, which is due to the accelerations and slow-downs of the activity implied by the trading time.

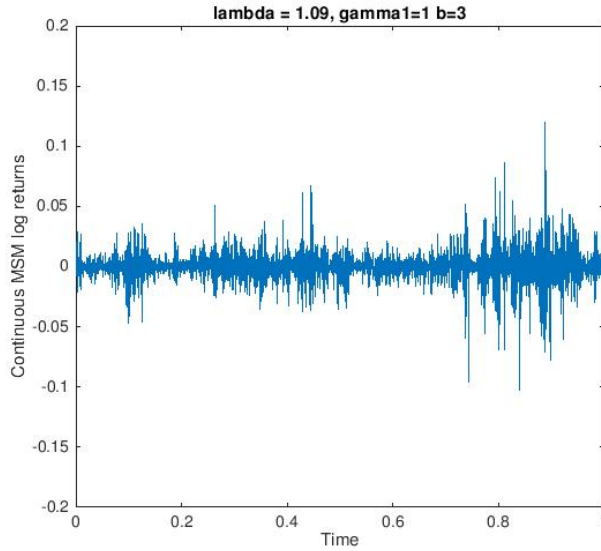


Figure 21: Returns obtained with the Continuous MSM with $k=10$ components. We have chosen $b=2$, $T=1$, $\gamma_1 = 1$, and a log-normal distribution M such that $\log_b(M) = \mathcal{N}(\lambda - 1, 2(\lambda - 1)/\ln b)$ where $\lambda = 1.09$.

6 Practical applications

6.1 Calibrating the Markov-Switching Multifractal in Discrete Time

6.1.1 Maximum-likelihood estimation

To calibrate the MSM in Discrete Time, we will use a maximum likelihood estimation. Assuming the financial series we study follow the MSM in Discrete Time with M having a discrete distribution between a finite number of values, what is left for us to do is to calibrate the model by determining the parameters m_0 , σ , γ_0 and b that best fit our series. We find these parameters by maximizing the Likelihood function, or in our case the log-likelihood function. For the MSM in Discrete time, this function is available in closed-form. The likelihood function considered as a function of our vector of parameters and given the set of returns of our financial series is the probability of obtaining these returns, considering they follow the Discrete Time MSM with this set of parameters :

$$L(r_1, \dots, r_t; \theta) \equiv \mathbb{P}_\theta(r_1, \dots, r_t)$$

with $\theta \equiv (m_0, \sigma, \gamma_0, b)$

We remind that \bar{k} is the number of components of the Markov-state vector M_t . Since the distribution M is discrete, the Markov State vector can take a finite number of values $m^1, \dots, m^d \in \mathbb{R}_+^{\bar{k}}$. We define the transition matrix $A \equiv (a_{i,j})_{1 \leq i,j \leq d}$ with $a_{i,j} \equiv \mathbb{P}(M_{t+1} = m^j | M_t = m^i)$. This transition matrix characterizes the dynamics of the Markov state vector.

Since we modeled the returns as $r_t = \sigma(M_t)\epsilon_t$ where ϵ_t are i.i.d. standard Gaussian variables $\mathcal{N}(0, 1)$, then we know that the return r_t has Gaussian density $f_{r_t}(r | M_t = m^i) = n[r; \sigma^2(m^i)]$ where $n(\cdot; \sigma^2)$ denotes the density of a centered normal random variable with variance σ^2 . However when calibrating our model, what we observe are the returns and not the Markov State vector. Thus, we are trying to compute the conditional probabilities:

$$\Pi_t^j \equiv \mathbb{P}(M_t = m^j | r_1, \dots, r_t)$$

We define the stacked row vector $\Pi_t = (\Pi_t^1, \dots, \Pi_t^d) \in \mathbb{R}_+^d$. By using Bayes' rule, we can compute the conditional probabilities Π_t recursively, by expressing it in function of Π_{t-1} and of the last return r_t :

$$\Pi_t = \frac{\omega(r_t) * (\Pi_{t-1} A)}{\omega(r_t) \cdot (\Pi_{t-1} A)}$$

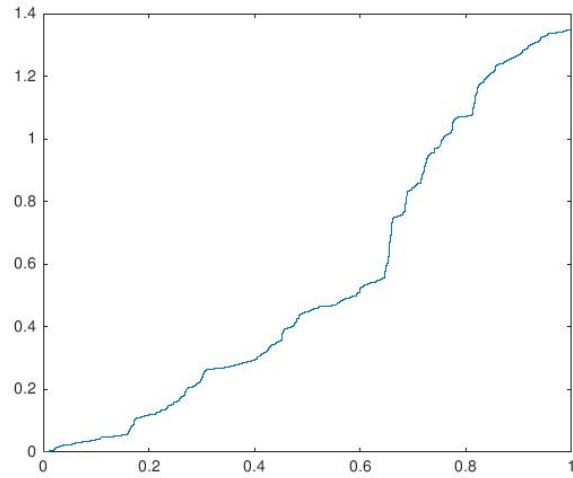


Figure 22: Trading-time of the Continuous MSM, obtained from the Markov components. We have $T=1$, $b=2$, $\gamma_1 = 1$, $\sigma_0 = 80$ and a log-normal distribution M such that $\log_b(M) = \mathcal{N}(\lambda - 1, 2(\lambda - 1)/\ln b)$. We have represented θ_k with $k=12$. As k tends to ∞ , θ_k converges weakly towards a multifractal time deformation θ_∞ . For implementation purposes, we have approximated $\theta_\infty = \theta_{12}$.

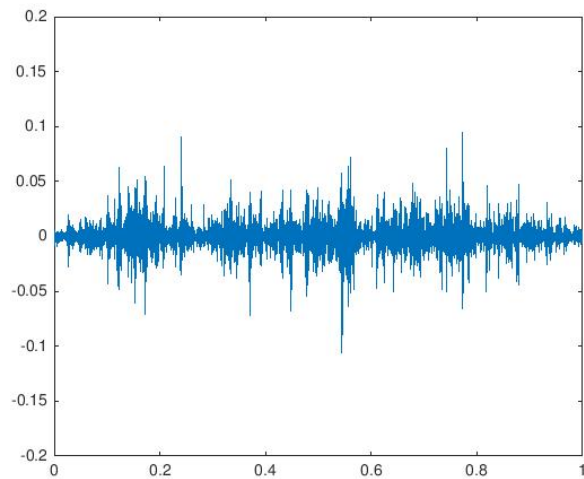


Figure 23: Returns obtained with the Continuous MSM with countably many components. We compounded a Brownian motion with the multifractal time deformation θ_∞ to obtain the log price $X(t) = B[\theta_\infty(t)]$, where $X(t) = \ln(P(t)) - \ln(P(0))$.

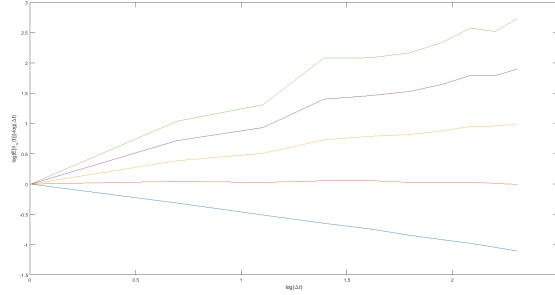


Figure 24: Moment scaling property of the the log-price process. We represented the $\text{Log}(\mathbb{E}(X(t))) - 1$ in function of $\text{log}(\Delta T)$. We made a Monte Carlo simulation over 400 paths of length 10000 for different time steps. As we can observe in this log-log representation, the scaling property seems to be respected as the plots are close to be linear. The different lines correspond to different moments: $q=0.5$ in blue, $q=1$ in red, $q=1.5$ in yellow, $q=2$ in purple and $q=2.5$ in green. The plots have been translated vertically to start at the point $(0,0)$.

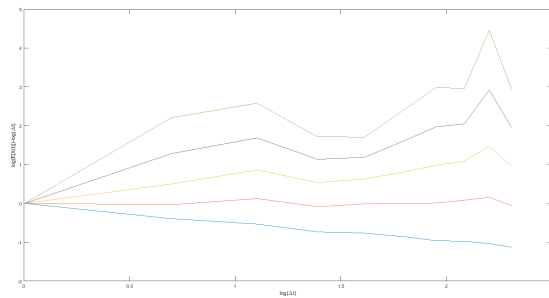


Figure 25: Moment scaling property of the trading time. We represented the $\text{Log}(\mathbb{E}(\theta_\infty(t))) - 1$ in function of $\text{log}(\Delta T)$. We made a Monte Carlo simulation over 400 paths of length 10000 for different time steps. As we can observe in this log-log representation, the scaling property seems to be respected as the plots are close to be linear. he different lines correspond to different moments: $q=1$ in blue, $q=2$ in red, $q=3$ in yellow, $q=4$ in purple and $q=5$ in green. The plots have been translated vertically to start at the point $(0,0)$.

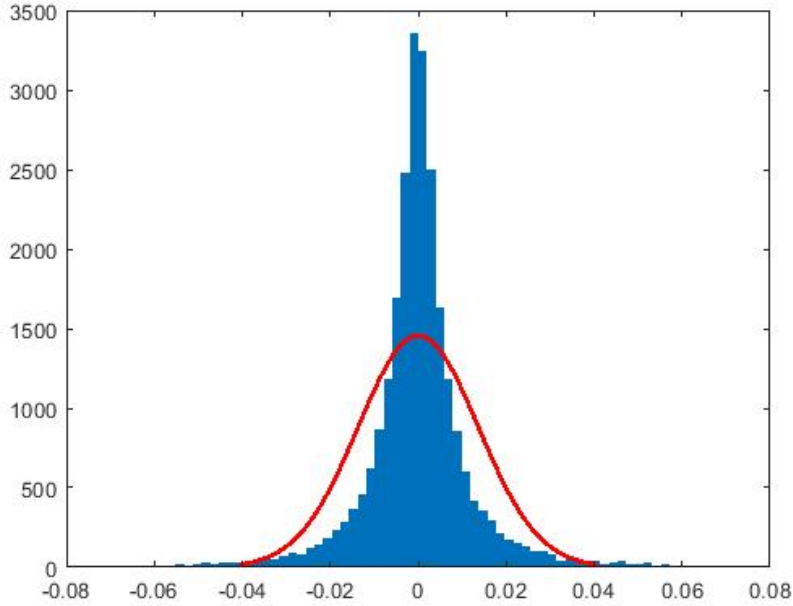


Figure 26: Distribution of the returns obtained with the MSM model with a countably many components, fitted by a normal distribution of the returns. We observe the tails are thicker for our model: accelerations and slow-downs in trading time affect the volatility, making it occasionally attain high levels.

where $*$ denotes the Hadamard product between two vectors: $x*y = (x_1y_1, \dots, x_dy_d)$ for all $x, y \in \mathbb{R}^d$, and $\omega(r_t) = (n[r_t; \sigma^2(m^1)], \dots, n[r_t; \sigma^2(m^d)])$. For the initialization, we set Π_0 to be equal to the ergodic distribution of the Markov process which is given, since the multipliers are mutually independent, by: $\Pi_0^j = \prod_{l=1}^{\bar{k}} \mathbb{P}(M = m_l^j)$ for all j .

Therefore, the closed-form log-likelihood is given by:

$$\ln L(r_1, \dots, r_T; \theta) = \sum_{t=1}^T \ln[\omega(r_t) \cdot (\Pi_{t-1} A)]$$

The objective is thus to find the vector of parameters θ that will maximize this log-likelihood function.

6.1.2 Practical results

We have calibrated the model by log-likelihood maximization on a data set of Canadian dollar - US dollar foreign spot exchange rate. The data set contains daily data, from January 4th 1971 to May 5th 2018.

By maximizing the log-likelihood, we obtain the following parameter values:

parameter	$\bar{k}=1$	2	3	4	5	6	7
m_0	1.99	1.70	1.64	1.58	1.52	1.49	1.44
σ_0	0.0281	0.0039	0.0044	0.0039	0.0039	0.0043	0.0040
b	1	37.0	71.7	12.1	7.24	9.06	6.29
$\gamma_1 (\times 10^{-3})$	0.0041	0.809	0.0249	0.113	0.0789	0.0089	0.0015
$\text{Ln L} (\times 10^4)$	5.08	5.41	5.44	5.45	5.46	5.46	5.48

As expected, the log-likelihood is a monotonic function of \bar{k} , because as k grows we allow more components to fit the variations of the volatility. Numerical test performed by Calvet and Fisher show that the log-likelihood usually reaches a maximum around $\bar{k} = 10$, and stays almost constant afterwards. We also observe that for $\bar{k} \geq 2$, the value of m_0 diminishes with \bar{k} : indeed,

as more components come into play, the fit is more precise with a lower discrepancy between m_0 and $2 - m_0$, so m_0 will get closer to 1.

In order to reduce the computational time, Calvet and Fisher proposed the following approximation: the parameter σ_0 can be set to be equal to the standard deviation of the returns in the data set, and the parameter γ_1 can be set equal to the inverse of the length of the data set. Thus, the first component should, on average, switch values only once during the length of the simulation. By making these approximations, we find the following results:

parameter	$k=1$	2	3	4	5	6	7
m_0	1.00	1.70	1.62	1.58	1.53	1.47	1.43
b	1	743	38.3	13.8	7.67	5.49	4.51
$\text{Ln L} (\times 10^4)$	5.08	5.41	5.44	5.45	5.46	5.46	5.46

Since the log-likelihoods are very close, we could indeed pursue with this approximation for further simulations.

6.2 Calibrating the Continuous Time MSM

6.2.1 Calibration using the multifractal spectrum

In the Continuous Time MSM, we recall that the parameters that we need to calibrate are the distribution M of the trading time θ_∞ , and the Hurst index of the log-returns. Unlike for the Discrete-Time MSM, the Continuous-Time MSM model does not allow us to find a likelihood function in closed form. Instead, we will use the properties of the multifractal spectrum to calibrate our model.

We start by partitioning the interval $[0, T]$ of our financial series into N intervals of length Δt , and we define the *partition function* as follows:

$$S_q(T, \Delta t) \equiv \sum_{n=1}^{N-1} |X(i\Delta t + \Delta t) - X(i\Delta t)|^q$$

If $X(t)$ is a multifractal and has finite q^{th} moment, the moment-scaling property holds $\mathbb{E}[|X(\Delta t)|^q] = c_X(q)(\Delta t)^{\tau_X(q)+1}$, and by applying the logarithm:

$$\ln \mathbb{E}[S_q(T, \Delta t)] = \tau_X(q) \ln(\Delta t) + c^*(q)$$

where $c^*(q) = \ln c_X(q) + \ln(T)$

We assume that the log-price follows $X(t) = B_H(\theta(t))$, that is the log-price is a Fractional Brownian Motion compounded with a MSM time deformation with countably many frequencies.

We remind the property that $\tau_X(1/H) = 0$. Thus, in order to identify the Hurst index H , the strategy we will use consists in plotting $\ln \mathbb{E}[S_q(T, \Delta t)]$ in function of $\ln(\Delta t)$ for several values, and observing the slope of the curve which is equal to $\tau_X(q)$. Although this property may not be exactly respected, it has been historically assumed that the log-returns follow a Geometric Brownian Motion, so we expect H to be close to $1/2$. This means that we expect the slope $\tau_X(q)$ to be close to 0 when q is close to 2.

Having determined τ_X , and therefore by taking its Legendre transform, we can determine the multifractal spectrum f_X of the log-price. By observing its graph, we can validate or invalidate the hypothesis we usually make, that is that the distribution of the multipliers M is lognormal, i.e. that the distribution of M is of the form:

$$-\log_b(M) \sim \mathcal{N}(\lambda - 1, \sigma^2)$$

Indeed, as we have seen in section 4.3.3, a process with multipliers having such a distribution has a multifractal spectrum of the form:

$$f_\theta = 1 - \frac{(\alpha - \lambda)^2}{4(\lambda - 1)}$$

and since in our model X is the composition of a fractional Brownian motion with the trading time $\theta(t)$: $X(t) = B_H[\theta(t)]$, then we have the relation between the multifractal spectra: $f_X(\alpha) = f_\theta(\frac{\alpha}{H})$. So, by noting $\alpha_0 = \lambda H$, we have

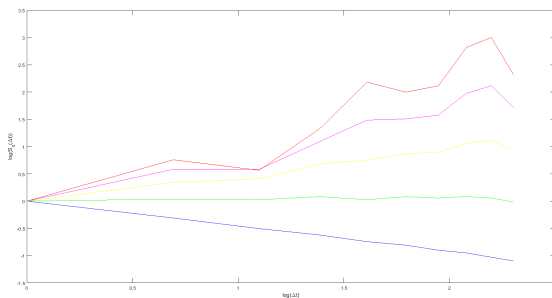


Figure 27: We represented the logarithm of the partition function of the log-exchange rate CAN-USD for several values of q , in function of $\log(\Delta t)$. In blue : $q=1$, in green $q=2$, in yellow $q=3$, in purple $q=4$ and in red $q=5$. We have translated these curves vertically so that they all start at the point $(0,0)$. As we can observe, these different curves are almost linear, so the scaling property of the partition function is indeed verified for this exchange rate. As expected for $q=2$, the curve is almost flat.

$$f_X = 1 - \frac{(\alpha - \alpha_0)^2}{4H(\alpha_0 - H)}$$

Thus, observing a parabola-shaped multifractal spectrum is an encouraging sign that indeed, the multipliers' distribution is lognormal.

By observing the parabola, we can identify the missing parameters of our distribution λ and σ . Indeed, we find α_0 by finding the point where the maximum of the parabola is reached, and since we have already identified H thanks to the scaling function τ_X , we obtain λ since $\lambda = \frac{\alpha_0}{H}$.

The base b of the multifractal process isn't uniquely defined by the spectrum alone, and we commonly assume $b=2$. Since $\sigma^2 = \frac{2(\lambda-1)}{\log(b)} = \frac{2(\lambda-1)}{\log(2)}$, we can also identify σ , and thus we have fully calibrated our model.

6.2.2 Practical results

We will study the Canada / U.S. foreign exchange rate, see if a model such as the Continuous MSM with countably many frequencies is appropriate to describe it and calibrate the model. Our financial series contains the daily exchange rate between January 4th 1971 and May 11th 2018.

In order to check if this multifractal modeling fits this financial series, we start by observing the scaling property of the partition function, see Figure 27. As we can see, this scaling property is verified for different moments, from $q=1$ to $q=5$. We can thus conclude that we can use this model to try to analyze our process. Moreover, as expected, the curve is almost flat for the moment $q=2$, which means that the process is close to the standard Brownian specification. Indeed, $\tau_X(1/H) = 0$ means that the Hurst index H is close to $1/2$. By doing an OLS estimation, we find that the slope is horizontal for $q = 1.942$, which in turn leads to

$$\hat{H} = 0.515$$

This index is an indicator of long-term autocorrelation. In our case, since $H > 0.5$, it means that our process is slightly persistent.

Therefore, we can deduce the scaling function of the log-price, that we represented in Figure 28. We observe that the function $\tau_X(q)$ is concave, which is an indicator of multifractality.

From the scaling function, we can deduce the multifractal spectrum $f_X(\alpha)$ after applying the Legendre transform. The multifractal spectrum has a parabolic shape, which is consistent with a log-normally distributed multiplier M .

The maximum is reached for

$$\hat{\alpha}_0 = 0.564$$

Since $\alpha_0 = \lambda H$, we find that

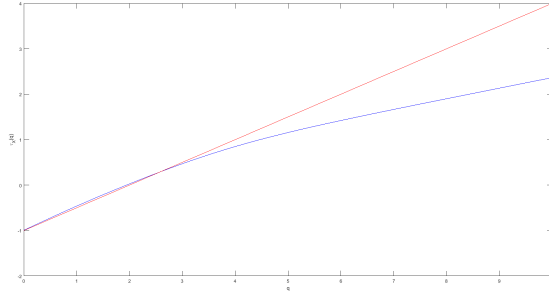


Figure 28: From the partition function, we deduced the scaling function τ_X , and represented $\tau_X(q)$ in blue in the graph. In red, we represented the line $y = 1/2x$, the scaling function of a process following a standard Brownian motion.

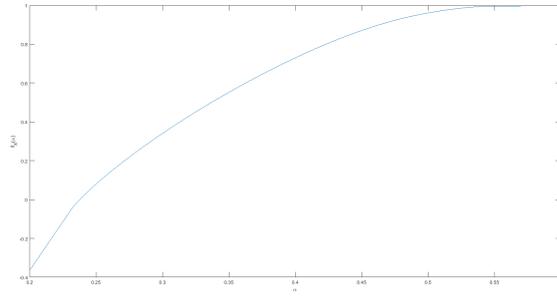


Figure 29: Multifractal spectrum $f_X(\alpha)$ of the logarithm CANUSD foreign exchange rate, obtained after applying the Legendre transformation to the scaling function $\tau_X(q)$. We observe that the multifractal spectrum has a parabolic shape, which is consistent with a log-normal distribution for the multiplier M .

$$\hat{\lambda} = 1.10$$

, and with the formula $\sigma^2 = \frac{2(\lambda-1)}{\log(2)}$, we find that

$$\hat{\sigma}^2 = 0.275$$

. So the calibrated process is of the form $X(t) = B_H[\theta(t)]$, with $\hat{H} = 0.564$ and a MSM time deformation with countably many frequencies $\theta(t)$ built with a multiplier M lognormally distributed, such that $-\log_2(M) = \mathcal{N}(0.1, 0.275)$.

7 Conclusion

In this thesis we have explored the use of Multifractals to analyze patterns in financial series. We started from an intuitive view of the time-scaling properties of the graphs of such financial series, before focusing on the intensity of the variations of the process and on the frequency of the repetition of these intensities.

To do so, we have defined mathematical objects such as the Hölder exponent of a function at a given point, which helps us measure the regularity of a function locally. Delving into the foundations of fractal geometry we have also defined the Hausdorff dimension of fractal objects, which is an indicator of the roughness of such an object. These two objects allowed us to define the multifractal spectrum f_X of a stochastic process X , which associates a given Hölder exponent to the Hausdorff dimension of the set of points where the process exhibits this exponent. The fundamental property of this spectrum is that it is the Legendre transformation of the scaling function of the process, which describes the behavior of the moments of the process as the time-step tends to zero.

We have afterwards defined three models exploiting multifractal properties : the Markov-Switching Model in discrete time and in continuous time, and the MMAR. The MSM in discrete time introduces the concept of Markov components of the volatility, which can change value at each time step with different probabilities. These probabilities can be associated to the frequency of switchings. The product of these different components is proportional to the volatility, thus the volatility is subject to the cyclic variation of these different components. This mimics the volatility of an asset in the real world, which is subject to the superposition of economic cycles with different time-length: long periods of calm can be locally subject to shorter period of relative unrest, the same way as we can observe long periods of market uncertainty. With the construction of the MMAR, we have used the mathematical properties of the binomial cascade to build a trading-time, which is a deformation of the time and defined as the cumulative distribution function of a binomial measure. This trading-time simulates the accelerations and slow-downs of the trading activity, which can be totally randomized in the case of a canonical measure. We obtain the MMAR log-price by compounding this trading time with a standard Brownian motion. Eventually with the Continuous-time MSM, we overcame the problem of the definition of the model on a time grid (MSM in discrete time) as the Poisson arrivals on the Markov components take place at random times. This model can have a finite number of components, or countably many components in which case we define a trading-time that weakly converges towards a multifractal process. To obtain the log-price, we can compound this trading time with a fractional Brownian motion. Moreover, we have shown for these three models that the properties of volatility clustering and long-memory are verified.

Finally, we have shown how to calibrate the MSM models, both in discrete and in continuous time. For the MSM in discrete time, we can calculate a log-likelihood function, which we can maximize in order to find the parameters of the model. In the case of the continuous time model, we have to find the Hurst exponent H of the fractional Brownian motion and the distribution of the multiplier used to build the components. We use the moment scaling properties of the process to find its scaling function, from which we can derive its multifractal spectrum which in turn helps us find the multipliers distribution. We have calibrated both of these models on the Canadian dollar - US dollar foreign exchange rate. We can note that in this thesis we have restricted ourselves to foreign exchange rate between strong currencies because of the symmetry they imply in the returns, which allows use a normal distribution of the returns in our model. For other cases, we could also include skewness in these distributions.

The multifractal models allow a description of financial series that incorporates properties that were overlooked by classic financial models. As larger and larger data sets are available and computational capacities have increased, the use of these models by practitioners has now become possible. They are however less simple to comprehend than classic models such as Black-Scholes as they require a certain familiarity with the mathematical concepts on which they rely.

References

- [1] Laurent E. Calvet, Adlai J. Fisher. *Regime-Switching and the Estimation of Multifractal Processes*. National Bureau of Economic Research, 2003.
- [2] Laurent E. Calvet, Adlai J. Fisher. *Multifractal Volatility: Theory, Forecasting and Pricing*. Academic Press Advanced Finance Series, 2008.
- [3] Laurent E. Calvet, Adlai J. Fisher. *Extreme Risk and Fractal Regularity in Finance*. Contemporary Mathematics, 2012.
- [4] J R Boer. *A comparison of GARCH and MSM Volatility Models*. Erasmus University Rotterdam, 2009.
- [5] David Harte. *Multifractals: Theory and Applications*. Chapman & Hall\CRC, 2009.
- [6] Kenneth Falconer. *Fractal Geometry: Mathematical Foundations and Applications*. John Wiley & Sons, 1990.
- [7] Benoît Mandelbrot. *Fractales, Hasard et Finance*. Champs Flammarion, 1997.
- [8] Benoît Mandelbrot. *How Fractals can explain what's wrong with Wall Street*. Scientific American, 2008.

8 Appendix

8.1 Appendix 1: The Hausdorff dimension of the Cantor Set

Let us prove rigorously that the Hausdorff dimension of the middle Cantor set is $\frac{\log 2}{\log 3}$

At each step $k \in \mathbb{N}$, the set E_k can be covered in 2^k sets U_i for $i \in 1, \dots, k$ of length 3^{-k} . Thus $H_{3^{-k}}^s(F) \leq \sum_{i=1}^k |U_i|^s = 3^{-ks} 2^k = 1$ if we let $s = \frac{\log 2}{\log 3}$. Thus, $H^s(F) \leq 1$ by letting $k \rightarrow \infty$. This also implies that $\dim_H(F) \leq \frac{\log 2}{\log 3}$, we now need to show the equality.

To do so, we will show that $H^s(F) \geq \frac{1}{2}$ for $s = \frac{\log 2}{\log 3}$. We will actually show that for any countable cover U_i of F , $\sum_{i=1}^k |U_i|^s \geq \frac{1}{2}$. We can assume these U_i are intervals and since F is compact, we can consider only finite covers U_i . For every U_i , there exists k such that

$$3^{-(k+1)} \leq |U_i| \leq 3^{-k}$$

Then U_i intersects at most one interval from E_k . For $j \geq k$, U_i intersects at most 2^{j-k} intervals of E_j . Using the previous inequality, $2^{j-k} = 2^j 3^{-ks} \leq 2^j 3^s |U_i|^s$. If we let j be big enough so that for all the U_i in our covering, $3^{-(j+1)} \leq |U_i|$. Since the covering U_i intersects all the 2^j intervals of E_j , this means since any U_i intersects at most $2^j 3^s |U_i|^s$ intervals of E_j , that $2^j \leq \sum_{i=1}^k 2^j 3^s |U_i|^s$.

By simplifying by 2^k , we obtain that:

$$\sum_{i=1}^k |U_i|^s \geq 3^{-s} = \frac{1}{2}$$

8.2 Appendix 2: Moment-scaling property of the log-price process for the MMAR and the MSM in Continuous time

In the MSM in Continuous time the log-price is a process of the form:

$$X(t) = B_H[\theta(t)]$$

In the case of the MMAR, $H = \frac{1}{2}$ so that the process is simply a composition of a standard Brownian motion with the trading time. In both models, the fractional Brownian motion and the trading time are independent processes.

$$\begin{aligned} \mathbb{E}[|X(t_1)X(t_2)|^q] &= \mathbb{E}\left[\mathbb{E}[|B_H[\theta(t_1)]B_H[\theta(t_2)]|^q | \theta(t_1), \theta(t_2)]\right] \\ &= \mathbb{E}[|\theta(t_1)^{qH} \theta(t_2)^{qH}|] \mathbb{E}[|B(1)|^q]^2 \end{aligned} \tag{1}$$

by independence of the processes.

Assuming here that the trading time autocorrelation declines hyperbolically, so does the autocorrelation of our log-price. The demonstration of the hyperbolic decline of the trading-time was done by Calvet and Fisher [2].